THE RETINAL TOPOGRAPHY OF THE RED LIONFISH (*Pterois volitans*): TOWARDS AN UNDERSTANDING OF THE VISUAL SYSTEM OF A HIGHLY INVASIVE SPECIES

by

© Juan P. Ibáñez

A Thesis submitted to the School of Graduate Studies in partial fulfillment of the requirement for the degree of

Master of Science, Cognitive and Behavioural Ecology

Faculty of Science

Memorial University of Newfoundland

August 2023

St. John's, Newfoundland and Labrador

ABSTRACT

Retinal specializations provide organisms with the spatial information needed to engage in visually guided behaviours aimed at maximizing fitness; nevertheless, little is known about the retinal topography of crepuscular fish, as most studies address diurnal or deep-sea species. I evaluated the types of photoreceptor and neural cells in the retina of the red lionfish, their distribution in the retinal surface, and their spatial resolving power. Single, double and triple cones are imbedded in a rod-dominated field over the entire inner layer. Single and double cones occur in higher densities towards the dorsal and ventral areas, arranged in a square mosaic pattern all along except in the central region of the retina, where they concur with triple cones. Ganglion and amacrine cells cover the outer layer with higher densities in the ventral-nasal region, a mismatch to single and double cones, and occasionally assemble as glomeruli or striation. Cell distribution and single and double cone arrangements in conjunction with spatial resolving power values suggest vision in *P. volitans* is adapted for vertically open habitats and performs better in dim-light environments while maintaining a moderate capacity for color vision, which denotes an advantage for predatory capabilities and success as an invasive species.

GENERAL SUMMARY

Vision in fish has been widely studied, although reef and deep-sea fish are the most researched groups. Through retinal topography, a visual representation of the structure, arrangement and sampling of retinal cells, I counted, produced maps and calculated the clarity of vision in cells that convert light into signals and send visual information to the brain in the red lionfish (*Pterois volitans*). I discovered that these cells are more abundant in the upper and lower regions of the retina, and they are organized in a way that grants the red lionfish the ability to see in environments where light levels are low, such as turbid or deeper waters. This benefits the capability of the fish to detect and pursue its prey, which, in addition to other biological and ecological factors, makes it a highly successful invasive species.

ACKNOWLEDGEMENTS

I acknowledge that the lands on which Memorial University and Universidad Jorge Tadeo Lozano's campuses are situated are in the traditional territories of diverse Indigenous groups. I acknowledge with respect the diverse histories and cultures of the Beothuk, Mi'kmaq, Innu, and Inuit of the province of Newfoundland and Labrador (Canada) and of the Kogi, Arhuaco, Wiwa, and Kankuamo of Santa Marta region (Colombia).

I thank my supervisor, Dr. Pierre-Paul Bitton for his constant guidance, experience and patience, and the members of my supervisory committee, Dr. Hélène Paradis, Dr. Maxime Geoffroy and Dr. James Drover (Memorial University), and Dr. Matteo Santon (University of Bristol) for their feedback.

Many additional people contributed to this project. Adolfo Sanjuan was a key ally and research supervisor at Universidad Jorge Tadeo Lozano. Andrés Pardo (Universidad Jorge Tadeo Lozano), Dr. Julian Prieto (formerly Universidad Jorge Tadeo Lozano), Dr. Sonja Knutson and Chris Hibbs (Memorial University) provided bureaucratic support, making inter-institutional cooperation possible -a specially challenging achievement during COVID times. Drs. Brian Cohn and Lars Schmitz were of great help in understanding and troubleshooting the retina R script. Dr. Sue Walling and Alex Burke provided methodological insight into wholemount and staining procedures. Javier Torres and Makarela diving center hosted scuba diving excursions, allowing me to observe my study species in the wild. Folks at CABE, especially the members of Dr. Bitton's Visual Ecology lab, were always around to maintain a friendly environment at "The Zoo".

Finally, my family. There will never be enough words or gestures to thank them for their limitless encouragement and support in all stages of my personal and professional life.

Table of Contents

List of Abbreviations

ACC	Animal care committee
cpd	Cycles per degree
DC	Double cones
GA	Ganglion and amacrine (cells)
KOH	Potassium hydroxide
LAD	Lionfish aggregation device
LED	Light-emitting diode
NGO	Non-governmental organization
PBS	Phosphate buffer saline
PND	Posterior nodal distance
PVC	Polyvinyl chloride
SC	Single cones
SPR	Spatial Resolving power
TC	Triple cones

List of Tables

List of Figures

List of Appendices

1. INTRODUCTION

1.1 An Overview of Visual Systems in Vertebrates

No matter how primitive or sophisticated, animal eyes are adapted to match the tasks they serve. Evolution of visual systems encompasses four main stages in accordance with any behaviour that may lead to an impact on fitness (Land & Nilsson, 2012; Nilsson, 2009):

1) Unshielded photoreceptor cells relate to behaviours controlled by non-directional monitoring of ambient light, such as the control of circadian rhythms, light-avoidance responses for protection against intense light, shadow responses to avoid predation, and surface detection for burrowing animals.
2) Pigmented ocelli with broadly directional photoreceptors induce behaviours based on directional light sensitivity, such as phototaxis, control of body posture (optical statocysts), and alarm responses for approaching predators (Figure 1).
3) Pigment pit or cup eyes with coarse spatial vision allow visual tasks based on low spatial resolution, such as detection of self-motion, object avoidance responses (anti-collision), habitat selection, and orientation to coarse landmarks or major celestial objects such as the sun or moon (Figure 1).
4) Eyes with focusing optics and high spatial resolution are ideal to perform visual tasks based on high spatial resolution such as detection and pursuit of prey, predator detection and evasion, mate detection and evaluation, orientation to fine landmarks, visual communication, and recognition of individuals (Figure 1).

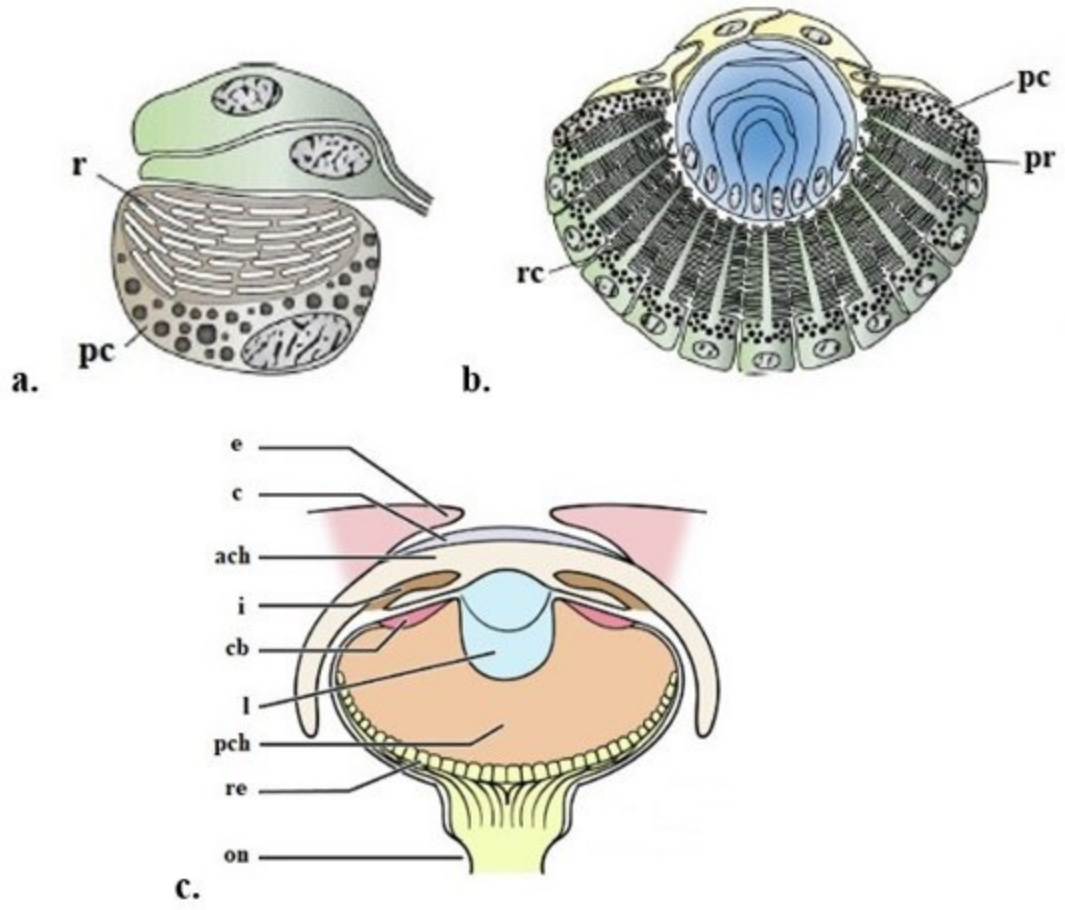

Figure 1. Schematic representation of ocelli and eyes of different stages of evolution in reference to items 2-4 above. Item 1 not included because unshielded photoreceptors are morphologically inconspicuous. a. ocellus of acoel flatworm; b. everse lens eye of juvenile box jellyfish; c. camera eye of common cephalopod. r: reflective crystals, pc: specialized pigment cell, rc: receptive cilium, pr: screening pigment, e: eyelid, c: cornea, ach: anterior chamber, i: iris, cb: ciliary body, l: lens, pch: posterior chamber, re: retina, on: optic nerve (Mallatt & Feinberg, 2021; Nilsson, 2009). Ocellus of acoel flatworm and everse lens eye of juvenile box jellyfish image © 2009 The Royal Society; cephalopod eye © 2021 Mallatt and Feinberg. All images modified from original sources under open-access Creative Commons Attribution License CC BY.

The eyes of vertebrates share many similarities with those of highly evolved invertebrates, as it is the case of the camera eye of cephalopods and humans as a result of convergent evolution (Ogura et al., 2004). Adaptive variations in the complexity of lenses, number of receptors, screening pigments, membrane stacking, and focusing optics capabilities respond to behavioural tasks in more evolved organisms (Land & Nilsson, 2012). Depending on the amount of spatial information an organism must deal with, either low-resolution or acute vision is required; hence, more complex visual tasks imply a higher need for faster receptors with narrower angular sensitivity and higher contrast sensitivity leading to a higher rate of photons capture (Land & Nilsson, 2012). Light spectral sensitivity refers to how efficiently an organism or a specialized device can detect light or other signals, as a function of their frequency or wavelength, while image resolution refers to the amount of detail an image might hold, which directly depends on the ability of the imaging system (Levine & Shefner, 1981). In essence, all eyes are constrained by the trade-off between these two properties. The quality of the image perceived by the retina, the innermost layer of tissue, is affected by numerous elements in the eye anatomy which may induce scatter, diffraction, and wavefront aberrations or errors (Applegate et al., 2003; Spadea et al., 2016).

As light enters camera eyes (e.g., Figure 1, Item 4), it refracts in the cornea and lens, focusing as a ray that travels onto the back of the eye, reaching the retina. The amount of light in the retina is determined by the shape and size of the eye and/or pupillary aperture (Cronin et al., 2014; Douglas & Djamgoz, 1990). Depending on the clarity of the ocular media, a portion of this passing light may be scattered, forming haze that is superimposed on the retinal image (Spadea et al., 2016).

The retina is the most advanced structure towards a high level of visual sensation. It consists of layers of neural tissue, ‘an extension of the brain’, responsible for mapping the visual environment of a particular species (Collin, 1999). A range of retinal specializations have been described in the retina, including variations in photoreceptor and neural cell number, density, arrangement, type and spectral sensitivity (Collin & Shand, 2003), and the presence and location of several types of ocular reflectors (Fritsch et al., 2017). The type, size, number and distribution of the different neural cells shape the visual system at the retinal stage (Walls, 1942).

The first level of visual sensation in the retina is achieved by photoreceptors located in its posterior layer, consisting of rods and cones. While rods mediate vision in dim-light conditions and induce visual responses to moderate contrast stimuli, cones moderate vision in bright-light conditions, accomplishing a major role towards color vision (Lamb, 2013; Tikidji-Hamburyan et al., 2017; Yokoyama, 2008). Photoreceptors can vary in length and width, and in the case of the cones, can be further divided into different morphological subtypes: single, double (two single cones fused together), triple or even quadruple cones (Ali & Anctil, 1976; Engström, 1963). An important cue for understanding eye evolution is the distinction between different types and distribution of photoreceptor cells, some of which are linked to early diversifications of photoreceptor physiology (Land & Nilsson, 2012).

Oil droplets in the inner segment of the photoreceptor layer filter the light spectra before it reaches light sensitive opsin proteins in the outer segment (Siebeck et al., 2003; Thorpe et al., 1993; Wilby & Roberts, 2017). Lastly, in the anterior level of the retina, intermediary neurons undertaking specific functions characterize the following level of processing before visual information reaches the cerebral cortex. Horizontal cells allow lateral communication between rods and cones, bipolar cells send electrical impulses to the ganglion cells, the main link to the

optic nerve, located in the inner layer of the retina, and amacrine cells, which precede the ganglion cell layer, allow lateral communication between them (Dowling, 2002). Nearly 40 different types of amacrine cells have been identified in the vertebrate retina; although their functional diversity remains understudied, they vary in terms of polarization/depolarization of main light spectra (e.g.: red vs. green, blue vs. yellow, yellow vs. blue; Thoreson & Dacey, 2019). Ganglion cells, on the other hand, consist of four different types: midget cells mediate red-green color vision and high-acuity color vision, parasol cells contribute mostly to the perception of motion, small bistratified cells mediate blue-yellow color vision, and wide-field cells are reactive to light or motion (Marshak, 2009; Yamada et al., 2005). Receptive field in ganglion cells ultimately sets the upper limit of visual acuity as well as the optical sensitivity of the eye (de Busserolles et al., 2020; Warrant & Locket, 2004).

1.2 Understanding the Ecology of a Species through Retinal Topography

Across layers of retinal tissue, photoreceptor population represents independent data points to collect visual information, while ganglion cells can sum this information before high-level processing in the brain (Collin, 2008). Retinal topography, that is, the representation of structure, arrangement and sampling of retinal cells, is an ideal method to visualize the spatial distribution of either photoreceptor cells or neural cells across the retinal surface. As a result of thorough dissection, wholemount and image processing techniques, topographic maps are obtained from cell counts measured across a regular sampling grid and displayed as an isodensity surface plot within a wholemount outline (Ullmann et al., 2012). The distribution of retinal cells should be at least somewhat different for each species.

In modern medicine, retinal topography represents an important resource to study retinal characteristics in eyes with common disorders or diseases such as myopia (Oh et al., 2014), cataract (Kim et al., 2018) and atrophic age-related macular degeneration (Shahidi et al., 2002), among others.

In the fields of behavioural ecology and veterinary sciences, retinal maps closely reflect the symmetry of perceived worlds, providing information on the role vision plays in animals' behaviour (Collin, 1999). Retinal topography is ideal to identify photoreceptor densities in determined locations of the eye, known as retinal specializations, which are key to understanding the relation between a species' environment and its behaviour. The following are the most described retinal specializations:

- *Area centralis*: a concentric increase in retinal cell density
- *Horizontal streak*: an elongated increase in cell density across the retinal horizontal meridian
- *Vertical streak*: an elongated increase in cell density across the retinal vertical meridian
- *Foveae*: deep and shallow pit-like structures, sometimes featured in area centralis or horizontal/vertical streaks

The presence of certain specializations, along with the overall distribution and density of photoreceptors and neural cells, also allow researchers to determine anatomical estimates of spatial acuity, which differs but is related to behavioural estimates.

Research on retinal topography supports close relationships between the physical nature and complexity of a species' habitat and the characteristics of its visual system. An *area centralis* -or fovea centralis in vertebrates in which the area is highly developed- allows high resolution,

binocular vision, for prey and object tracking (Rapaport & Stone, 1984). Species that frequent an open environment or an uninterrupted view of their horizon present a band-shaped increase in retinal cell density across the horizontal meridian or horizontal streak (Collin, 1999; Hughes, 1977), while vertical streaks are more common in species that climb trees, mountains or migrate vertically (Collin, 2008). Animals who feature a fovea are mainly predators, such as raptor birds or fish that engage in strike tactics, as they require local image resolution and/or movement detection (Potier et al., 2017; Webb, 1984).

According to Collin's review on retinal topography (1999), of all five classes of vertebrates, fish were the most studied taxa by the late 20th century; a trend maintained in current scientific literature. Visual specializations may differ between teleost species and/or within the eye itself depending on the visual ecology, environment, and/or phylogenetic inertia of each species (Carleton et al., 2020; Collin & Pettigrew, 1989; Cronin et al., 2014; Dalton et al., 2017; de Busserolles & Marshall, 2017; Stieb et al., 2019). Since teleost fishes inhabit a broad range of environments with different light conditions and structural complexity, have different activity patterns, diets, and display a variety of behaviours, their visual systems meet different visual demands and therefore play a crucial role in communication, prey detection, predator avoidance, habitat choice, and/or navigation (Collin & Marshall, 2003; Walls, 1942).

1.3 Lifestyle and Vision in Fishes

In general terms, although examination of retinal specializations shows an increase in central density of all cell populations relative to peripheral densities, most studies on retinal topography have concentrated on either photoreceptor or ganglion cell populations (Collin, 1999).

Previous work with birds by Lisney et al. (2012, 2015, 2020) demonstrated several patterns that coincide with other vertebrates' lifestyles:

- Eye shape and retinal topography vary among species in relation to different activity patterns and habitat preferences.
- The central and temporal areas of high neuron density allow for increased spatial resolution in the lateral and frontal visual fields, respectively. Increased resolution in the frontal field in particular may be important for mediating feeding behaviors that require precise movements in small-scale spaces.
- Eye morphology and retinal topography may reflect a cathemeral activity pattern and the physical nature of the habitats in which some animals live.

As stated previously, fish -including agnathans, cartilaginous and bony fish-, are currently the group of vertebrates that has been subject to most retinal topography studies. There is, in fact, a high tendency towards studying the visual systems of diurnal inhabitants of coral reefs rather than those of nocturnal species, due to these ecosystems' characteristic brightness and colorfulness. Although, as an example among uncommon exceptions, there is confirmation of the visual system of squirrelfishes being well adapted to their nocturnal lifestyle with a rod-dominated retina (de Busserolles et al., 2020).

Cryptobenthic (from the Greek *kryptós* meaning "hidden") organisms are those that inhabit the seafloor and spend most of the time hiding under caves or crevasses or relying on some sort of camouflage to prevent predation and/or capturing their prey by ambush (a.k.a. sit-and-wait predators; Goatley & Brandl, 2017). Retinal topography on the triplefin blenny *Tripterygion*

delaisi (Fritsch et al., 2017), a crypto-benthic species with a micro-predatory lifestyle determined the following main features:

- Single and double cones are more abundant in the dorsal and temporal area culminating in an *area centralis* with a distinct fovea.
- Single and double cones dominate the retina and are consistently arranged in a mosaic pattern, which may facilitate color vision since the change in ratio in the foveal region suggests sensitivity boosts in relation to the rest of the retina, and motion detection as the species could notice minute movements and track the source to focus with the fovea.
- Retinal ganglion cells follow photoreceptor distribution across the retina but form no distinctive pattern.
- Location and resolving power of the fovea would benefit the detection and identification of small prey in the lower frontal region of the visual field, although further studies are needed.

The first retinal map performed on the black scorpionfish -and on any scorpaeniform to my knowledge- *Scorpaena porcus*, demonstrated retinal characteristics that coincide with its predatory crypto-benthic lifestyle (Santon et al., 2018). This species features four photoreceptor types: rods, single, double and triple cones that are present in a higher density both in the periphery of the retina and as a horizontal streak towards the nasal region and distributed randomly near the falciform process (Goudie, 2019). There was no assessment of retinal ganglion cells or neural cells of any type.

1.4 Problem Statement, Purpose Statement and Research Question

The Scorpaeniformes (Pisces) are a diverse order of carnivorous ray-finned fish that typically have spiny heads, rounded pectoral and caudal fins are and mostly distinguished by the presence of a suborbital stay -a backwards extension of a part of the lateral head skeleton (Paxton et al., 1998). The order is composed of around 35 families including Scorpaenidae (scorpionfish, lionfish), Triglidae (searobins), Platycephalidae (flatheads), Gasterosteidae (sticklebacks) and Cyclopteridae (lumpfishes) among others; taxonomic classification is not settled (Nelson et al., 2016). Scorpaenids (i.e. Scorpaenidae family) includes venomous species, which present spines – most commonly dorsal, anal and pelvic- coated with venomous mucus (Paxton et al., 1998).

Scorpaenids feature a wide variety of habitat selection and predatory strategies, which rely on the structure and efficiency of their visual system. Although much research has been conducted on retinal topography for cryptobenthic fish, there is still little known on scorpaeniforms and nothing particularly focused on lionfish species so far. The red lionfish (*Pterois volitans*) has gained high relevance as an invasive species in the Colombian Caribbean during the last decade (Pabón & Acero, 2016). Any additional knowledge that may lead to a deeper understanding of its ecology and behaviour is of great importance, as it contributes to the improvement of management and invasive species mitigation plans.

Pterois volitans (Linnaeus, 1758) is a medium-size fish (usually ≤ 35 cm total longitude) with conspicuous dorsal and pectoral fins featuring large and strong venomous spines and a white and reddish pigmentation stripe pattern on its skin (Freshwater et al., 2009; Halstead et al., 1955; Hernández-Abello et al., 2014) (Figure 2). This species inhabits coral reefs, rocky bottoms, seagrass prairies among other ecosystems among solid structures in the bottom of the oceans, such as rocks or submerged logs, soft and hard bottoms, from 0 to 120 m depth (Ureña, 2009;

Whitfield et al., 2002). Due to its eye-catching aspect, the red lionfish is very popular amongst aquarium owners, which makes them easy to find worldwide (Freshwater et al., 2009). Intentional and accidental release, in some cases due to natural disasters (e.g., hurricanes), as well as natural dispersion (Kletou et al., 2016; Whitfield et al., 2002) have contributed to lionfish invasion.

Figure 2. Red lionfish *Pterois volitans*. The species features zebra-like skin pigmentation, long spines and protuberances at the corners of the mouth. Photo: Denys Razumosvskyi under free-access Pexels license.

Although the red lionfish is endemic to the Indo-Pacific Ocean, there have been reports in the United States' East coast since 1992, spreading to the Bahamas towards 2004 and to most Caribbean Nations by 2007-2008 (Chevalier-Monteagudo et al., 2008; Guerrero & Franco, 2008; Morris et al., 2008; Whitfield et al., 2002; Whitfield et al., 2007). Its occurrence in the

Colombian Caribbean was documented for the first time in 2009, more particularly in San Andres and Providencia Archipelago and Santa Marta Bay region (González et al., 2009) (Figure 3). Due to its large impact as an invasive species in the Caribbean and the Atlantic coast of North America, it has become a threat towards local biodiversity (Freshwater et al., 2009; Whitfield et al., 2002) as well as to economic activities (Pimentel et al., 2000). This is not different in Colombian waters, as fishing communities in the Caribbean Sea have been impacted by the presence of the lionfish. From personal conversation with local anglers in the region, I have gathered knowledge on how fishermen along the Colombian Caribbean coast and insular territories tend to believe lionfish are responsible for the decreasing in their harvest, as it preys on local species that are of traditional and commercial importance. Anglers are also afraid of capturing and consuming the lionfish due to its venomous characteristics. Nevertheless, several Non-Governmental Organizations (NGOs), environmental entities, superior education institutions and others have addressed this issue with the purpose of educating the communities and providing them with the knowledge and tools to incorporate the lionfish as part of their traditional diet. This would encourage indiscriminate capturing of the lionfish, hence, promoting a potential mitigation to its invasive populations.

The red lionfish features widely competitive traits such as its spines that serve as protection against potential predators, abilities such as a water squirting technique used to stun its prey (Albins & Lyons, 2012), and generalist feeding habits that have led to a drastic reduction to diverse reef fish populations (Pabón & Acero, 2016). Additionally, its wide dispersion (1-300 m depth, 18-30º C, pH 8-8.5, 30-40 ppm salinity in early reports) and environmental tolerance (5-7 ppm salinity) in experimental setups (Jud et al., 2015), high fecundity, larval survival rate and colonizing persistence, has provided this fish with an enormous success as an invasive species

(Côté et al., 2013; Lasso et al., 2010). As I will address further in this document, this species frequents dark environments and maintains great predatory efficiency in the absence of light(Côté & Maljković, 2010; Morris, 2012). An approach to the characteristics of its visual system will lead to a greater understanding on the visual mechanisms of the species, to a deeper understanding of social and predatory behaviour as well as to potential implications for its management as a highly invasive species.

What type of photoreceptor cells are present in the retina of the red lionfish, how are photoreceptor and ganglion cells distributed along the retinal surface, and what is the spatial resolving power for both types of cells? The purpose of this research project is thus to describe retinal specializations in my focus species. I intend to identify photoreceptor and ganglion cells in my focus species, to estimate cell densities, distribution patterns and spatial resolving power for both photoreceptors and ganglion cells. Information on both types of cells is complementary by nature, as they are involved in the path of light before it reaches the brain and should provide a more accurate estimation of visual capabilities.

Therefore, I will estimate photoreceptor and ganglion cell densities in the retinal surface of the red lionfish in order to:

- Produce retinal maps representing cell photoreceptor and ganglion cell distribution in the outer and inner surface of the retinal tissue respectively, since photoreceptors and ganglion cells occur in opposite sides, as well as possible alignments between photoreceptor and ganglion cell distribution.
- Establish ratios such as single-to-double cone or ganglion-photoreceptor ratio.
- Identify specific cell configuration patterns within the retinal tissue.

- Estimate the species' spatial resolving power (i.e., spatial resolution).

Any numeric data and identification of visual features obtained through this methodological procedure along with bibliographical research will be relevant to discuss possible relationships between visual and behavioural adaptations.

Previous work towards vertebrates in general and specific aspects of scorpaeniforms allows one to consider a series of hypotheses in relation to the red lionfish's photoreceptor diversity, density and distribution that may provide a deeper insight on several ecological aspects:

1) During their juvenile and developing stages, lionfish seek shelter and prey in coral reefs, mangrove forest and other shallow-water environments but tend to move to greater depths as they grow larger (Morris, 2012). I expect a greater photoreceptor density in a vertical fashion, either by a vertical streak per se or clustering in the dorsal and ventral areas of the retina, which would allow the species to perceive light coming from above as efficiently as possible in downwelling light environments, low daylight exposure (e.g., dusk and dawn), or greater depths.

2) Lionfish have the ability to blow jets of water to disorient prey fish and strike fast (Albins & Lyons, 2012). Hence, retinal mapping may address spatial orientation by either a concentric gathering (i.e. *area centralis*) or vertical display of photoreceptors distribution, and the clearest possible image in relation to light levels, considering the fact that the species prefers low or dim-light environments (Côté et al., 2013).

2. METHODS

2.1 Specimen Collection

Twenty red lionfish individuals of sizes ranging from 7.50 cm to 19.80 cm standard length were captured by local fishermen in Santa Marta Bay (Magdalena, Colombia; Figure 3) and transported to the Universidad Jorge Tadeo Lozano (UTADEO) laboratories. I maintained the specimens at UTADEO facilities in captivity, extracted, hemisected, and preserved the eye samples for further dissection and analysis at Memorial University.

Figure 3. Colombian Caribbean Coast and Insular territories. Yellow circle in the center-right: Santa Marta Bay; large grey rectangle in the upper-right: San Andrés and Providencia Archipelago. Source: Google Maps

I kept fish specimens in groups of 8-10 individuals in 500 l containers maintained at a temperature of 20-26˚C, salinity of 25-35 ‰ and pH 8.1-8.4, corresponding to average values in

the area. The containers were covered by a plastic lid with small openings to allow light to pass through, maintaining a dim-light environment (Figure 4). After 2-3 days of conditioning after collection, I provided the lionfish with live small local fish (e.g., sardines, mackerel) and shrimp as food source once a week and cleaned the containers with the same frequency.

Figure 4. Plastic containers for lionfish (left); lionfish and live prey inside container (right). Containers include solid objects such as PVC tubes, plastic nets and coral skeletons to provide shelter and air stones for constant oxygen supply. Photo credit: Juan P. Ibáñez.

All stages of sample extraction and retinal wholemounting were performed following the wholemount protocol proposed by Ullman et al. (2012) with slight modifications. To prepare specimens for eye extraction, I moved each individual to a 15 l aquarium (Figure 5) completely covered by a plastic container to prevent light from entering, conditioning the fish to a dark environment for a period of 2 hours as minimum as a means to minimize tissue stress, as indicated in the protocol. After the dark-adaptation period was over, I anesthetized the fish by adding clove oil solution, consisting of ethanol (C_2H_5OH) and clove oil in a 9:1 ratio, to a relative

volume of 20 ml for 10 l of salt water for 20 min before euthanizing them by pithing.

Figure 5. Individual aquarium for dark-adaption and anesthetizing. The aquarium appears uncovered to display the conditions for the fish to be anesthetized. Photo credit: Juan P. Ibáñez.

2.2 Sample Extraction

Before and during eye extraction, I registered morphometric parameters that would be useful for comparison purposes, such as specimen standard length and head width, corneal diameter, eyeball transverse length, eyeball axial length, lens equatorial diameter and lens transverse diameter. I did not perform any sort of sexual differentiation, since the red lionfish does not have notorious sexual dimorphism, and I did not assess sexual maturity levels based on gonadal development.

I used a data collection sheet to register every step of the procedure (see Appendix A), eye characteristics and measurements, as well as time in reagents, and took photographs at each stage.

2.2.1 Eye Enucleation

I cut the conjunctiva using small scissors with curved blades, pulled the eye out of the orbit with forceps and cut adipose tissue, extraocular muscles, the optic nerve and any remaining connective tissue (Figure 6). Once each eye was removed, I measured the corneal diameter and the transverse and axial lengths using calipers.

2.2.2 Opening the Eyeball

I punctured the eyeball slightly above the ora serrata and made an incision at the limbus to allow cutting along the edge of the cornea and iris and to remove corneal surface to reveal the lens. As a guide for maintaining the orientation of the eye and the retina after extraction (Figure 6), I made a small cut at the dorsal edge. I pulled the lens upwards, cut it free of retractor/protractor lentis muscles and measured the equatorial and transverse diameter of the lens using calipers.

2.2.3 Eyecup Fixation

I immersed each eyecup in 4 % paraformaldehyde in 0.1 M phosphate buffer saline (PBS) for 1.5-2 h depending on the size of the eye (Ullmann et al., 2012). After removal from the fixative, I removed the excess of solution by dipping the eyecup in PBS while gently grasping the optic nerve. I washed each eyecup three times for one minute in PBS. All eyecups were stored in previously labeled plastic containers filled with PBS at 4˚C and eventually transported to Memorial University of Newfoundland St. John's campus for the subsequent steps of the protocol.

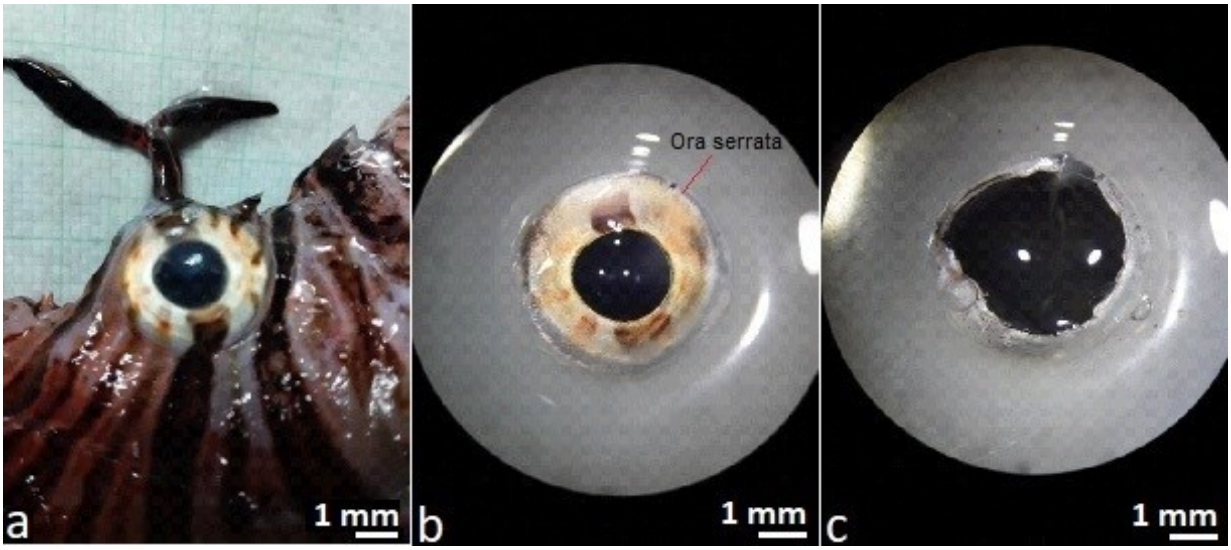

Figure 6. a. Lionfish eye close-up; b. enucleated lionfish eye; c. eyecup/hemisected lionfish eye (right). Photo credit: Juan P. Ibáñez.

2.2.4 Retinal Extraction and Wholemounting

I extracted the retinas and produced the retinal wholemounts following the steps indicated in Appendix B. During the retinal extraction procedure, I submerged each eyecup sample in a petri dish containing 0.1 M PBS to avoid dehydration or further decaying of the tissue. I removed the remaining vitreous humor, cut the outer layer of sclera, peeled back the choroid later and removed any remaining portion of optic nerve using a fine hair paintbrush.

I made small cuts along the periphery of each retina to reduce tension and allow them to lie flat more appropriately. I then immersed the samples in a bleaching solution consisting of 0.1 M PBS, 30 % H_2O_2 and 1.0 M KOH in a 9:1:8 ratio for 15-30 min with the purpose of removing the remaining retinal pigment epithelium. Ratio of reagents in the solution is the standard in the protocol, while the length of time required depends on the amount of epithelium remaining, while

avoiding not damaging the tissue due to long exposure to corrosive agents (i.e., KOH). I rinsed the samples in PBS three times to remove any residues of bleaching solution before wholemounting.

To avoid squishing the photoreceptors when making each wholemount, I glued spacers made of filter paper to microscope slides using nail varnish. Since photoreceptors are located in the outer layer of the retina, I placed samples facing down (vitreal surface down) in microscope slides. I added a few drops of 80 % glycerol as mounting medium, before covering and sealing the slides with varnish. I labelled each slide with the species name, an identification code, the type of sample (retina in glycerol), my initials and the date of wholemount.

Some of the samples were damaged during the dissection process while others were merely used to set and standardize retinal extraction protocols. I selected six final samples corresponding to three left eyes and three right eyes for photoreceptor counting and reused four of them to process and stain for Ganglion cell counting.

2.3 Visual Analysis

2.3.1 Generating Sampling Locations

I captured images of the wholemounted retinas using a Northern Light Model R95 transilluminator light box linked to an Imaging Retiga 2000R camera and a Sigma DG macro lens. I then uploaded the pictures in ImageJ v1.53a (Schneider et al., 2012), where I outlined each retina, saved the outline as a ROI file and displayed a grid across this outline. As the obtained grid allows equal sampling at regular distance interval, I considered the intersections of the gridlines inside the retinal outline as sampling (cell counting) locations, with approximately 200

locations per retina in accordance with Ullmann *et al*. (2012) (Figure 7), and registered these intersections in an x, y coordinate system.

Position of retinal landmarks such as the optic nerve head or the falciform process are important for the interpretation of retinal maps, hence, the coordinates of these landmarks are required for the mapping process. My samples featured a falciform process in form of an elongated opening from the center towards the ventral pole of the tissue which served as orientation landmarkI obtained the coordinates on the falciform process of each retina using the same tool to indicate sampling locations.

2.3.2 Photoreceptor Cell Counting

I performed visual processing of each retinal wholemount by means of a light microscope (Olympus BX51) attached to a digital camera (Olympus UC90) and a lens (Olympus U-TV1x-Z) supported by imaging software Olympus cellSens Entry 3.2. I observed each sampling location at a magnification of 400x and highlighted an area of 50 µm x 50 µm where I was able to identify and count all types of cone photoreceptors in a way to estimate densities, reported in cells/mm^2. I did not estimate rod density due to their small size, which makes them extremely challenging to identify and count by other means than electron microscopy. I registered noticeable distribution patterns among cones by capturing screenshots, and by means of a known scale, estimated photoreceptor diameters (single and triple cones) or major and minor axes (double cones) and distances between double cones when relevant, to provide averages in areas of different densities.

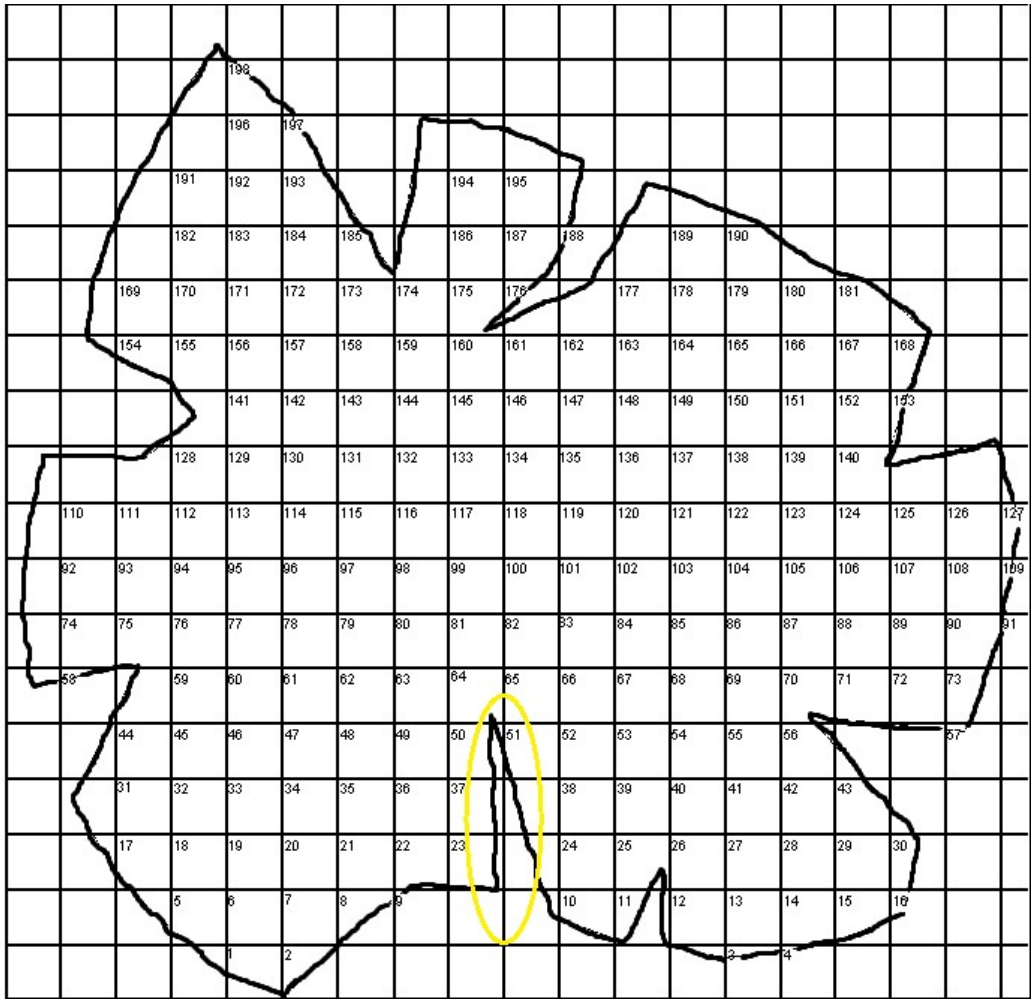

Figure 7. Grid and sample locations within an example retinal outline with 198 sampling locations (location #1 on the bottom left; location #198 on the top left). The most ventral opening corresponds to the falciform process (yellow circle). Other openings in the outline correspond to cuts or tears to facilitate flattening of the tissue.

2.3.3 Ganglion Cell Counting

Ganglion cell counting can be performed on new retinal samples or retinal wholemounts previously used for photoreceptor counting, as was the case in this study. I disassembled the retinal wholemounts by sliding a scalpel under the cover slip to crack it and remove it while

making sure not to damage the retinal tissue and removed the retinae by soaking the slide in 0.1 M TRIS buffer and applying some pressure with a fine paintbrush. I washed each retina in PBS three times for 5 min each (Ullmann et al., 2012), immersed them in a new container with PBS and placed them in new slides previously gelatinized slides, facing up -as opposite to for photoreceptor cell counting- since ganglion cells are located in the frontal part of the retina. Next, I rotated the retina on the slide to make sure the orientation was consistent with the position of the eye in the skull and the orientation of the former wholemounts. I observed the new slides by means of a dissection scope, flattened the retina using a fine paintbrush, measured the retina with a ruler (as a first set of measurements to estimate possible shrinkage) and placed the slides aside to dry overnight before staining.

I performed the staining procedure by following the standard Nissl stain protocol at the Neuroscience laboratories at Memorial University (Appendix C). This protocol consists mainly in staining the tissue of interest by means of Cresyl Violet, which highlights structural features of neurons in a blue-purple coloration, through dehydration and rehydration by means of acetic acid, acetone, xylene or derivative reagents. As the final step, I covered the slides using Permount® mounting medium, left them to dry for 24 hours before analysis and took a last measurement to determine tissue shrinkage.

Due to their similar morphology and nature (neural an interneural respectively) and their high densities, I counted ganglion and amacrine cells indistinctively; hence, I will mainly refer to them as GA cells from this point on. Using the same microscope, camera and software as for photoreceptor counts, I identified and counted GA cells at a magnification of 400x in an area of 20 μm x 20 μm per counting location. Since GA cells are considerably smaller than cones (see Figures 10 and 12), a smaller counting area was sufficient to estimate density and total population

in the overall retinal surface. GA cells were abundant in the retinal surface, making it very challenging to obtain an accurate count. I estimated cell densities over an area set in the less clustered region in each counting location taking tissue shrinkage in consideration, as the total retinal surface area in samples used for GA cell counting became smaller because of the staining process. I recorded all the cell counts and other relevant information in a table template which included the species, the specimen ID, eye side (right or left), counting points, counting point coordinates and number of GA cells.

2.3.4 Generating a Retinal Map

I used RStudio Version 1.2.5033 (R Development Core Team, 2014) to generate the final version of retinal maps by entering three files which feature 1) the retinal outline (ROI file), 2) the counting points, coordinates and counts for each type of cell (.csv file) and 3) the falciform process coordinates (.csv file). The R package Retina (Cohn et al., 2015), specifically developed to facilitate the visualization of cell densities across retinal wholemounts of chambered eyes, allowed the drawing of iso-density contours to generate a map featuring the cone type and density and the position of natural landmarks (i.e., the falciform process) within the retinal outline in accordance to the retinal orientation. The steps to obtain a retinal map from the first picture of the retinal wholemount through this R script are described in Appendix D, Figures 15 D1 and 16 D2.

2.3.5 Spatial Resolving Power

I determined the spatial resolving power for both photoreceptors and GA cells by means of Matthiessen's ratio, the standard way to calculate spatial resolving power for teleosts (Collin & Pettigrew, 1989), as described next and detailed in Appendix E.

The distance from the center of a lens to the retina or posterior nodal distance (PND) is 2.55 times the radius (r) of the lens and can be estimated after measuring the lens transverse and equatorial diameter during the eyeball hemisection procedure (see Appendix B). The angle (α) subtending 1 mm on the retina is equal to the arc tangent of 1 mm divided by the PND. Spatial resolving power is then calculated by obtaining the number of cells subtended by 1 degree of visual arc, that is, the calculated peak density divided by the PND. Lastly, since a minimum of 2 cells are necessary to distinguish the dark and light boundaries that make up 1 cycle of grating of the highest resolvable frequency, the spatial resolving power is obtained by dividing the estimated cells per degree by 2 and expressed in cycles per degree (cpd).

2.4 Ethics and Animal Care Statement

Since the red lionfish is considered as invasive in Colombian territory, no collection or manipulation permit was required; as for Memorial University's institutional guidelines, all procedures regarding this project followed ACC Animal Use Permit 19-04-PB.

3. RESULTS

3.1 General Eye Features

I processed 20 red lionfish ranging from 7.5 cm to 19.8 cm standard length for retinal dissection and wholemounting; the largest eye had a transverse length of 11.4 mm while the smallest one was 5.3 mm (Table 1), both corresponded respectively to the largest and smallest individuals.

Table 1. Morphometric parameters based on N = 20 individuals. SL: standard length; HW: head width; CD: corneal diameter; TL: eyeball transverse length; AL: eyeball axial length; ED: lens equatorial diameter; TD: lens transverse diameter

	SL (cm)	HW (cm)	CD (mm)	TL (mm)	AL (mm)	ED (mm)	TD (mm)
X	14.21 ± 3.04	2.23 ± 0.38	3.9 ± 0.81	8.31 ± 1.51	5.16 ± 1.18	3.11 ± 0.81	3.12 ± 0.75
Max	19.8	2.77	5.65	11.4	7.45	5.3	5.2
Min	7.5	1.25	2.2	5.3	3	1.8	2

Of 40 eye samples (20 left and20 right eyes), only six were suitable for retinal wholemounting - three for each eye. Table 2 presents the morphometric parameters of the six specimens from which the final samples were obtained.

The iris features a typical yellow-brown axial stripes pattern over a white and light yellow background, with dark brown pigmentation between the dorsal and ventral surfaces (Figure 6). The eye has a circular pupillary aperture with no aphakic gap, no eyelids or other protective structures other than the conjunctiva.

After enucleation, hemisection and removal of the lens, the hemicup inner surface is fully covered by the retinal pigment epithelium as the first layer of tissue before reaching the retinal epithelium and the *stratum argenteum* -a reflective cellular layer located in the outer choroid- right after.

Table 2. Morphometric parameters of red lionfish specimens used for retinal mapping. ID: sample identification label; SL: standard length; HW: head width; CD: corneal diameter; TL: eyeball transverse length; AL: eyeball axial length; ED: lens equatorial diameter; TD: lens transverse diameter

ID	SL (cm)	HW (cm)	CD (mm)	TL (mm)	AL (mm)	ED (mm)	TD (mm)
Pv09L	12.90	2.40	3.50	8.20	4.70	3.10	2.70
Pv11L	16.40	2.49	4.05	9.45	6.50	3.35	3.30
Pv11R	16.40	2.49	4.00	8.80	4.80	2.45	2.65
Pv19L	16.90	2.07	4.30	9.70	5.45	3.80	3.10
Pv19R	16.90	2.07	4.20	9.40	5.60	4.10	4.00
Pv20R	16.80	2.53	5.60	11.10	7.40	5.30	4.70

3.2 Photoreceptors

I found four types of photoreceptors in the red lionfish's retina: rods, single cones, double cones and triple cones. Rods vastly dominated the overall retinal surface, although, as previously mentioned, due to their reduced size -in comparison to cones- and the large amount all over the retina, I did not consider them for mapping and posterior discussion of findings.

3.2.1 Single Cones

Single cones were observed in the entire retinal surface with an average count of 3378.28 $\pm$ 1261.48 cells/mm^2, a maximum of 12800 cells/mm^2 and an estimated total population of 500 000 cells, average estimated surface coverage of 150.99 mm^2 and an average diameter of 3.36 $\pm$ 0.50 µm for the six samples processed for retinal wholemount and mapping (Table 3). Their densities

were relatively higher on the dorsal and ventral areas, though decreasing towards the center in a round-edged triangle.

3.2.2 Double Cones

Double cones were also found all over the retinal surface and are the most abundant type of photoreceptor in the red lionfish retina. I estimated an average count of 7612.31 $\pm$ 2143.91 cells/mm^2, a maximum of 21200 cells/mm^2 and total population of over 1100000 cells in a retinal surface coverage of 150.99 mm^2 for the six final samples (Table 3); featuring a rather oval shape, height and width measured 6.95 $\pm$ 0.48 μm and 3.46 $\pm$ 0.43 μm respectively. They displayed a similar array as single cones, with higher densities on the dorsal and ventral areas.

3.2.3 Triple Cones

With an average count of 1773.33 $\pm$ 1089.99 cells/mm^2 and a maximum count of 4800 cells, triple cones -consisting of three circular cones of similar size clustered in a central point- were only found in 15 fields across the six retinas (Table 3). They were considerably less abundant and their distribution along the retinal surface was more limited than for single and double cones. The average diameter considering the distance from the middle outer edge of one cone cell to the intersection of the two adjacent ones was 6.73 +0.67 μm, and they were only present around the optic nerve and along the falciform process in direction to the ventral pole. Due to their limited occurrence, I did not estimate the total population in relation to the retinal surface.

Table 3. Summary of stereological parameters and data, based on N = 6 individuals, Area 96.04 mm^2; N sites 1176; Area sampling fraction 0.63

Cell type	Cell counts/Sampling locations	Mean density (cells/mm^2)	Maximum count (cell/mm^2)	Total cell population	Size
Single cones	1176/1217	3378.28 ± 1261.48	12800	43 000 000	3.36 ± 0.50 µm
Double cones	1176/1217	7612.31 ± 2143.91	21200	161 000 000	Length 6.95 ± 0.48 µm Width 3.46 ± 0.43 µm
Triple cones	15/1217	1773.33 ± 1089.99	4800	8 500 000	6.73 +0.67 µm

3.2.4 Retinal Map and Cone Distribution Patterns

Due to the relatively high abundance of single and double cones, I was able to generate maps for each of these types of photoreceptors (Figures 8-9), their added densities (Figure 10) and their relative (i.e., double-to-single cone) ratio (Figure 11). Retinal topographic maps derive from the azimuthal projection of a flat plot to a spherical plot when processing the cell counts in the counting field coordinates in the Retina R package. Due to minor differences in the rotation of individual samples during the projection process, some structures and patterns are mispositioned in the resulting maps. As a reference for resulting photoreceptor maps, I selected the sample with the least noticeable rotation or misshaping for analysis purposes, without disregarding common features to all six maps.

Photoreceptor cells distribution consist of two *areae centrales* located in opposed regions of the retinal surface along a slightly (~25°) rotated vertical axis, which, due to morphologically mirror imaging, went clockwise in left eyes and counterclockwise in right eyes. Single and double cones occurred in a similar fashion: density was higher on the dorsal and ventral area; no fovea-type

clusters (Figures 8-9); the lowest counts corresponded to quartile-like positions and towards a central location, reaching the optic nerve. Relative densities of double to single cones increased from the central region to the temporal and ventral edges of the periphery and decreased towards the dorsal edge (Figure 11). This distribution indicates the eye holds higher visual resolution above the horizon of the visual environment.

The falciform process in the retina of the red lionfish was found in the ventral pole all the way to the center in a vertical position, connecting with the (now absent) optic nerve, as represented in figure 7 (see Methods). In figures 8 to 10 it is located diagonally towards the temporal pole due to rotation of the original coordinates. When observed in the light microscope, whenever only single and double cones were present in the same sampling location, they would feature a pattern previously described by other authors (see Discussion) as the "square mosaic pattern". The square mosaic pattern consists of a single cone surrounded by four double cones displaying a 2:1 ratio of double to single cones, with rods filling in the gaps between cones. This distribution was not always symmetrical and there were sometimes voids, as the central single cone was not always present and there was a prevalence of rods instead. This pattern had two variations in accordance with the spacing between cones edges of double cones across the central single cone or the voided area surrounded by double cones. In higher and lower density areas represented in the obtained maps, average distance between edges almost doubled, from 6.63 ± 0.65 μm to 12.45 ± 1.46 μm (Figure 12). When present, triple cones along with single and double cones occurred randomly, with no distinctive pattern but a 2:1:1 ratio where triple cones were the dominant type (Figure 13).

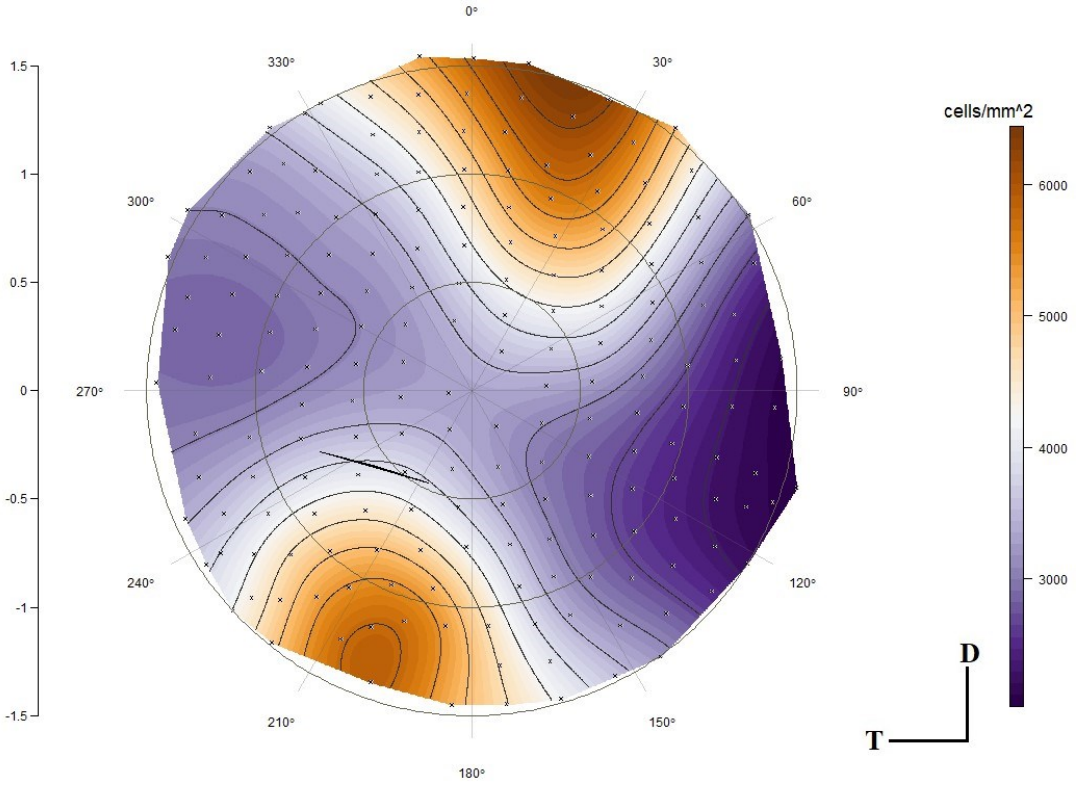

Figure 8. Retinal photoreceptor map showing the distribution of single cones in the left eye of a red lionfish individual of 12.90 cm of standard length with a corneal diameter of 3.50 mm and a retinal surface area of 113.09 mm^2. Since the retinal epithelium is located in the posterior part of the eye, the temporal and nasal pole are respectively located to the left and right side of the image. The black straight line towards the central region represents the falciform process. D: dorsal pole; T: temporal pole.

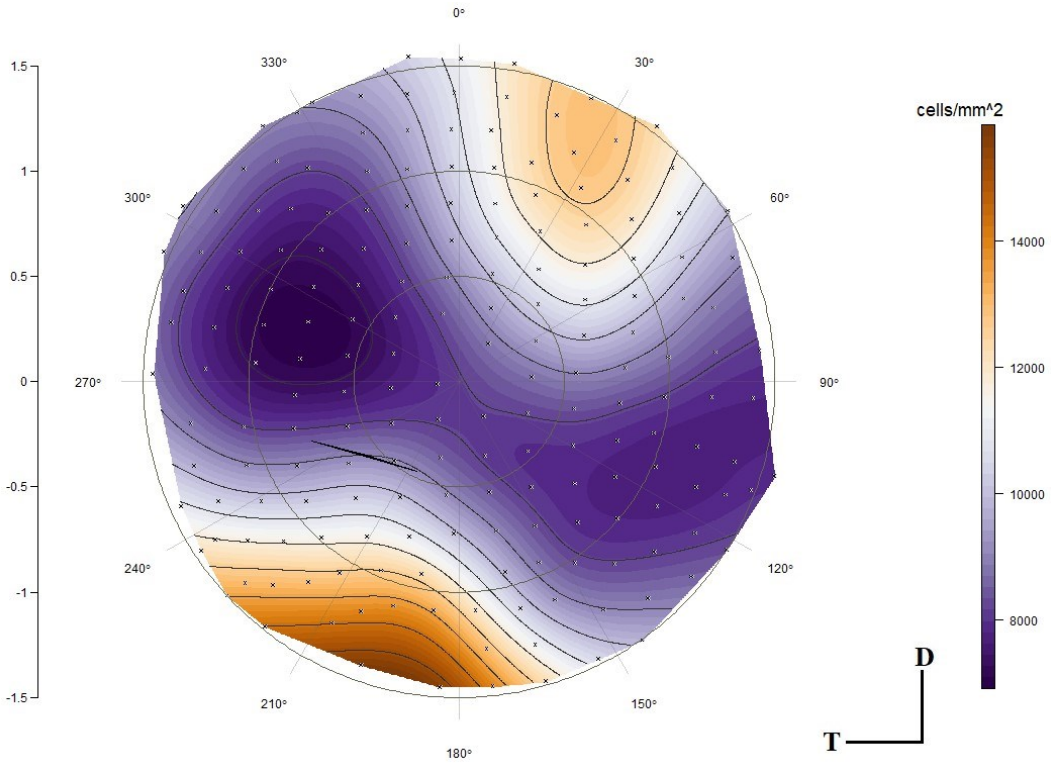

Figure 9. Retinal photoreceptor map showing the distribution of double cones estimated in the left eye of a red lionfish individual of 12.90 cm of standard length with a corneal diameter of 3.50 mm and a retinal surface area of 113.09 mm^2. Since the retinal epithelium is located in the posterior part of the eye, the temporal and nasal pole are respectively located to the left and right side of the image. The black straight line towards the central region represents the falciform process. D: dorsal pole; T: temporal pole.

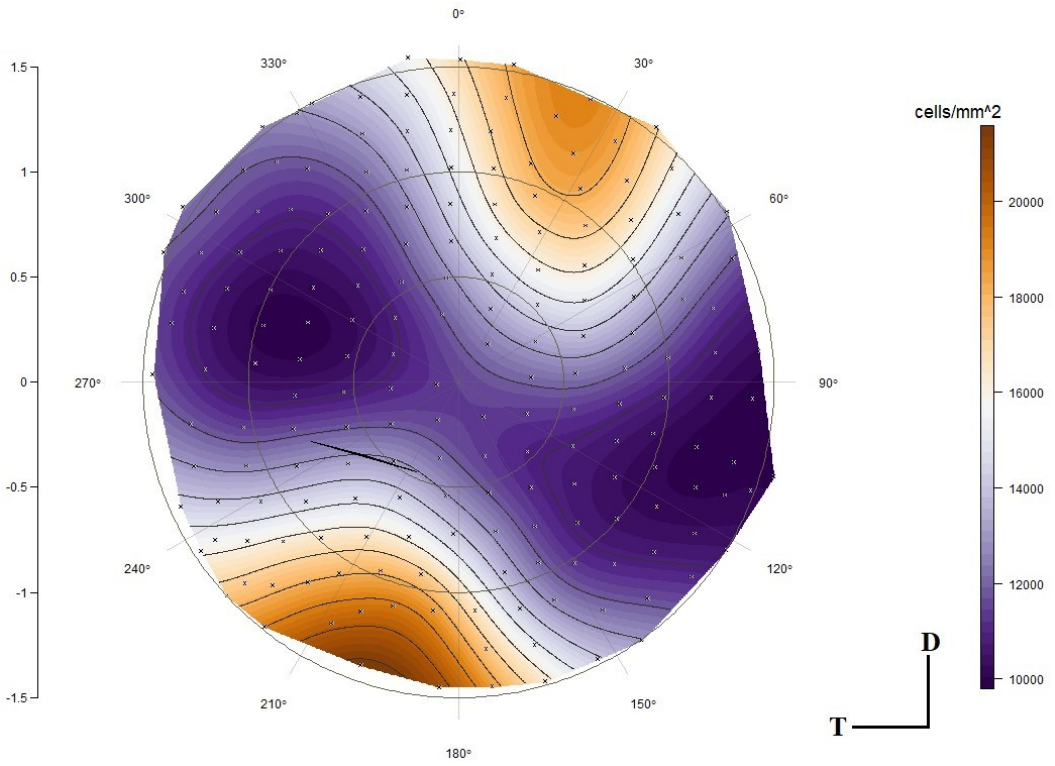

Figure 10. Retinal photoreceptor map showing the distribution of the estimated sum of single and double cones (down center) in the left eye of a red lionfish individual of 12.90 cm of standard length with a corneal diameter of 3.50 mm and a retinal surface area of 113.09 mm^2. Since the retinal epithelium is located in the posterior part of the eye, the temporal and nasal pole are respectively located to the left and right side of the image. The black straight line towards the central region represents the falciform process. D: dorsal pole; T: temporal pole.

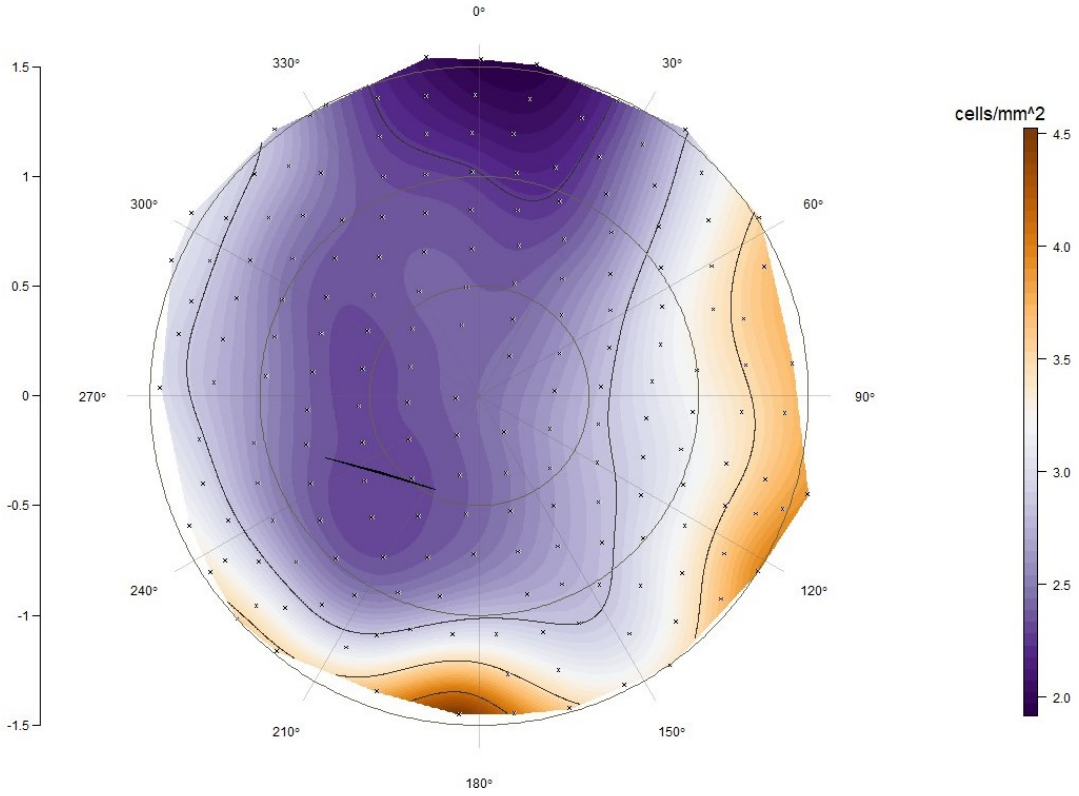

Figure 11. Retinal photoreceptor map showing the relative ratio of double to single cones, represented by the legend to the right (e.g.: 2.0:1.0 double cones for one single cone), in the left eye of a red lionfish individual of 12.90 cm of standard length with a corneal diameter of 3.50 mm and a retinal surface area of 113.09 mm^2. The black slightly diagonal line towards the central region corresponds to the falciform process. D: dorsal pole; T: temporal pole.

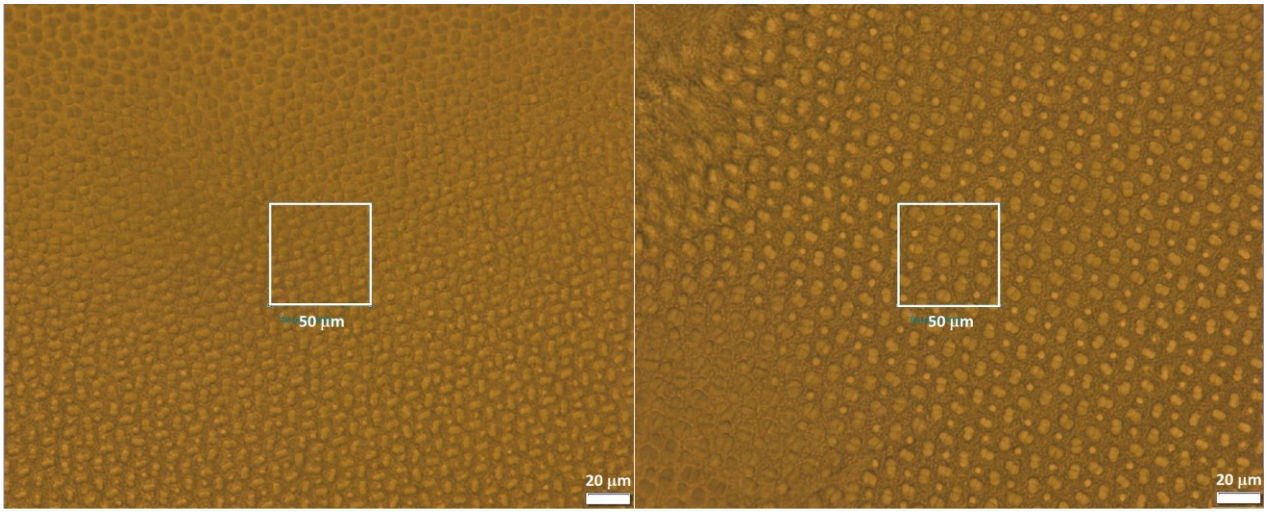

Figure 12. Single and double cones in a square mosaic pattern. Higher density area, smaller distance between double cone edges (right); lower density area, greater distance between double cone edges (left).

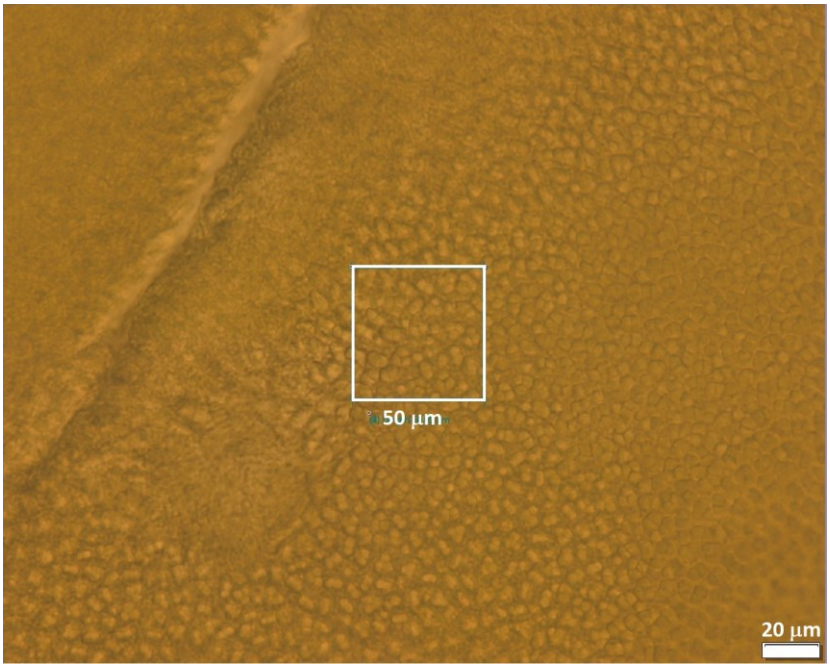

Figure 13. Triple cones along with single and double cones in a random disposition near the falciform process.

3.3 Retinal Ganglion and Amacrine Cells (GA cells)

Since photoreceptor and ganglion cells -as well as other intermediary neurons- exist in opposite sides of the retinal tissue, retinal wholemounts required disassembling, flipping of the tissue and staining for GA cell counting. Two of the four samples selected for GA cell counting suffered major damage during this process and were not suitable for counting. I was only able to obtain GA cell counts for two eyes -one right and one left.

GA cells were found all over the retinal surface with average and maximum densities of 49579.09 $\pm$ 13161.73 cells/mm^2 and 105000 cells/mm^2. Densities were higher towards the ventral-nasal region of the eye and considerably low in the dorsal surface (Figure 14); mirror imaging displays this trend towards opposite horizontal areas of the map. The falciform process was located at the ventral area, although it mispositioned when projecting the map to a circular plot, as seen in other maps.

GA cells were highly abundant in relation to single and double cones as a total. GA cell densities in nasal and temporal areas were three times greater than photoreceptor cells, 3.85 times greater in the dorsal area and up to 4.6 times in the ventral area (Figure 15).

GA cells occasionally gathered as glomeruli but mostly spread along the retinal tissue with a sporadic striation pattern, or no particular pattern at all (Figure 16). Due to the existence of areas of high agglomeration of GA cells, it was not possible to identify and hence determine the distribution of distinctive patterns within the retinal surface.

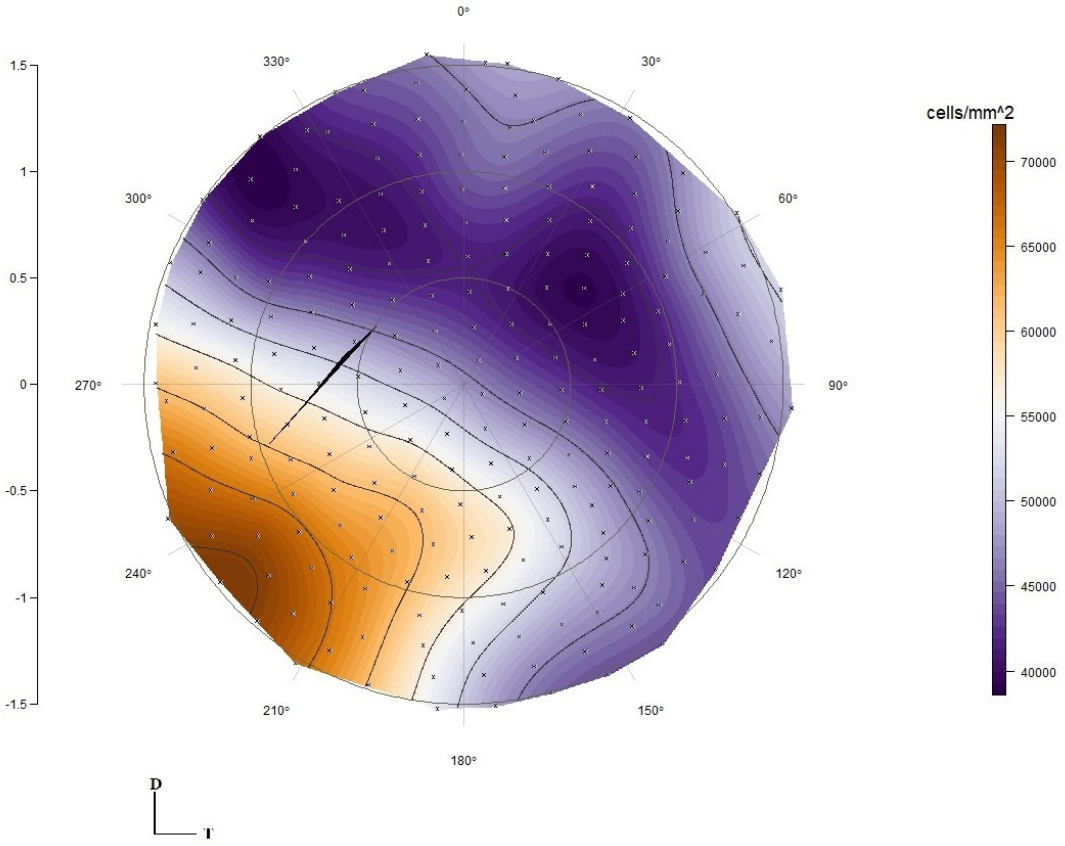

Figure 14. Retinal map showing the distribution and density of GA cells in the left eye of a red lionfish individual of 16.90 cm of Standard Length with a corneal diameter of 4.20 mm and a retinal surface area of 153.94 mm^2. Since the retinal epithelium is located in the frontal part of the eye, the temporal and nasal pole are respectively located to the right and left side of the image. The black spot represents the falciform process. D: dorsal pole; T: temporal pole.

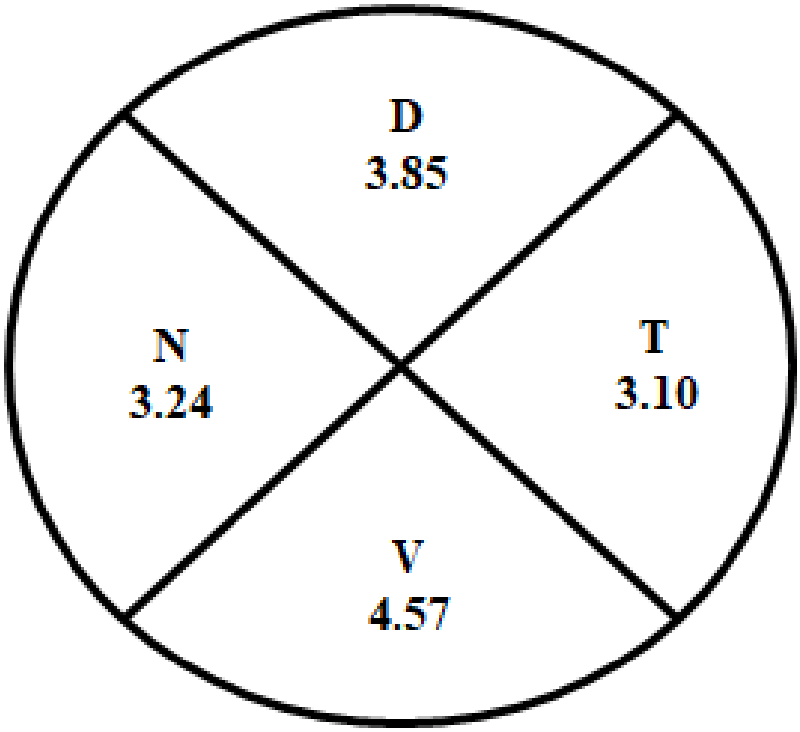

Figure 15. Schematic representation of average (N = 2) GA cells vs. sum of single and double cones ratios in the retinal tissue from a frontal perspective of a left eye (GA side). D: dorsal area; V: ventral area; N: nasal area; T: temporal area.

a.

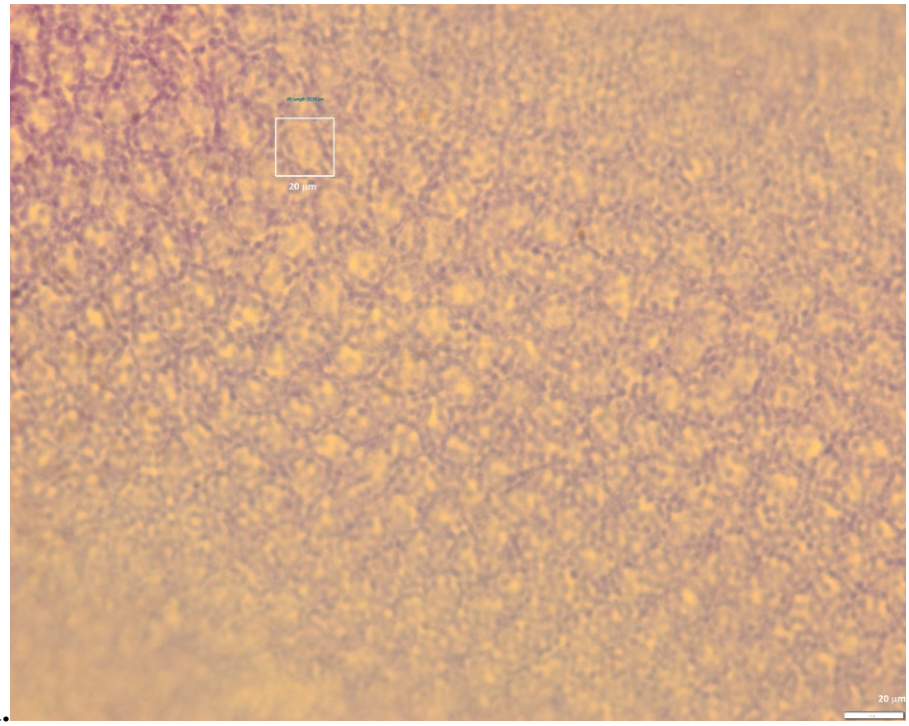

b.

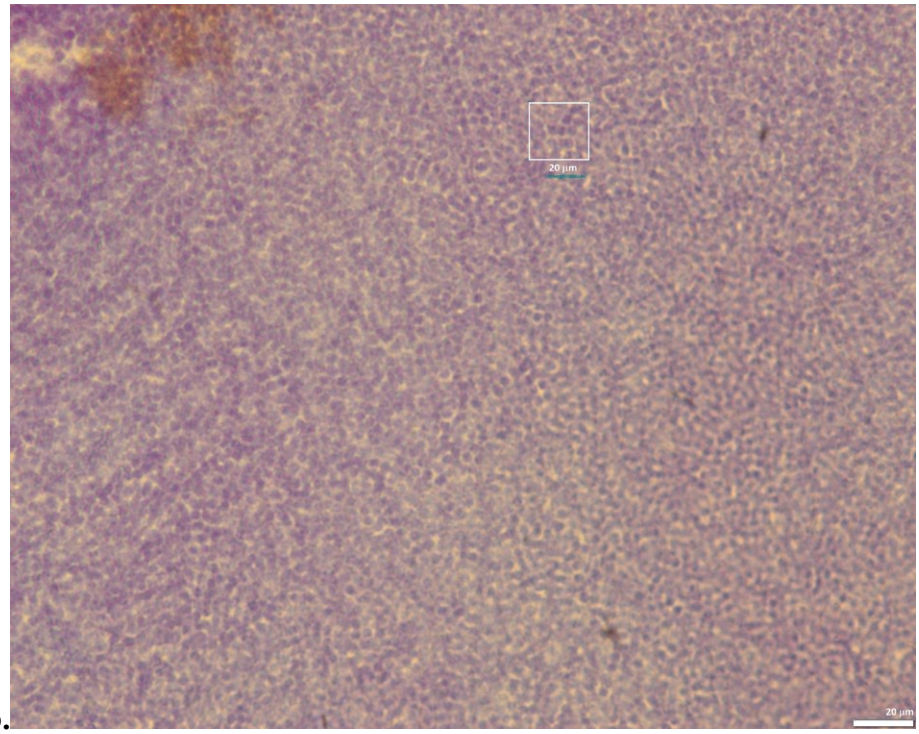

Figure 16. Ganglion and amacrine cells grouped as glomeruli; b. Ganglion and amacrine cells spread in striation.

3.4 Spatial Resolving Power

To estimate spatial resolving power, I used the lowest and highest added single and double cone densities of 17200 cells/mm^2 and 26400 cells/mm^2 in contrast to double cones counts of 11600 cells/mm^2 and 21200 cells/mm^2. These values were obtained from the specimen with the lowest and highest cell counts, of 19.80 cm of standard length and 5.6 mm of corneal diameter and 12.90 cm of standard length and 3.5 mm of corneal diameter, respectively. For GA cells, I used the lowest and highest densities of 12500 cells/mm^2 and 105000 cells/mm^2 from the same sample, obtained from a specimen of 16.60 cm of standard length and 4.20 mm of corneal diameter. I estimated the PND at 4.70 mm, based on the average lens radius of 1.84 $\pm$ 4.45 mm (N = 6) multiplied by 2.55, considered as the average Mathiessen's ratio for teleosts (Matthiessen, 1886). The resulting ranges of spatial resolving power were of 7.97-18.42 cpd under the conservative and the maximal assumption for photoreceptors, and 10.69-30.99 cpd for GA cells.

4. DISCUSSION

4.1 Results Summary

Out of 20 lionfish individuals dissected, I obtained six photoreceptor retinal maps and two GA cell maps. I found rods, single, double and triple cones in the retinal tissue; while rods were not included in cell counting, single, double and triple cones had average densities of 3378.28 $\pm$ 1261.48 cells/mm^2, 7612.31 $\pm$ 2143.91 cells/mm^2 and 1773.33 $\pm$ 1089.99 cells/mm^2 respectively. Rods, single and double cones occurred within the entire retinal surface while triple cones were only present following the path of the falciform process from the center of the retina towards the ventral pole. Single and double cones featured a typical square mosaic pattern with four double

cones surrounding a central single cone or no cone in some areas, where rods were clearly visible. Distance between double cones in this pattern was smaller in more dense areas (6.63 ± 0.65 μm) and greater in less dense areas (12.45 ± 1.46 μm). Single and double cones displayed a rather vertical distribution with greater densities displayed as *area centrales* towards the ventral and dorsal areas. Double to single cone ratios were higher towards the ventral and nasal edges of the retina. GA cells also occurred all over the retinal surface with an average of 49576.09 ± 13161.19 cells/mm^2 and displayed different patterns such as glomeruli and striations. It was not possible to determine an accurate distribution of these patterns within the retina due to some areas with cell agglomerations that did not allow performance of accurate counts or the identifications of certain arrangements. GA cells showed greater densities towards the ventral-nasal region of the eye, while GA cells to single and double cones ratio was higher in the ventral area, followed by the dorsal area, and slightly lower in the nasal and temporal areas. Spatial resolving power (SRP) was of 7.97-18.42 cpd for photoreceptors and 10.69-30.99 cpd for GA cells.

4.2 Photoreceptor Distribution, Cell Types and Patterns

4.2.1 Retinal Topography of the Red Lionfish

Topographic maps for the retina of the red lionfish demonstrate that cones are most abundant towards the edges, mostly in dorsal and ventral areas, and that double-to-single cone ratio is higher at the ventral and temporal peripheral edges (Figures 8-11). None of the available retinal topography map evaluated during this work describes photoreceptor vertical streaks as such, which would suggest they are uncommon in ichthyic species. Instead, dorsal- or ventral-positioned *areae centrales* are common depending on their habitat. Fritsch et al. (2017) described a dorsal-positioned *area centralis* in *T. delaisi*. Many lanternfishes (i.e. deep-sea fishes) instead

feature ventral-positioned *area centralis*, as reported by de Busserolles & Marshall (2017). The reef barrier anemonefish *A. akindynos* presents a central agglomeration with a ventral and slightly vertical spread (Stieb et al., 2019).

Retinal specializations establish the linkage between a species' environment and its behaviour. Species inhabiting environments with an interrupted horizon tend to have at least one area of high density (Shand, 1994), while species living in open environments usually have streaks (de Busserolles et al., 2014). In this context, the orientation of visual streaks corresponds to physical structures or landforms animals are associated to, such as trees to sloths and elephants (Collin, 2008) or activity-related behaviours, such as exploration or migration. While horizontal streaks featured in reef fish are considered a suitable adaptation for predatory surveillance or feeding behaviour when swimming in deep terraced reef fronts or areas of open water (Collin & Pettigrew, 1988b), vertical streaks are common in active vertically migrating deep-sea fish (Collin, 2008). In the regions of the retina where cones are less dense, spread out or scattered, objects tend to appear blurrier and with less vivid colors (Baars & Gage, 2012). A rather vertical spreading of photoreceptors, in accordance with my observations, suggests horizontal and/or peripheral vision is not a robust feature for the red lionfish but rather the ability to see below and above the horizon with outstanding accuracy. The red lionfish is not a migratory species per se; instead, it can occupy different depths as required, while swimming slowly, roaming and exploring new environments (Gress et al., 2017). Two *areae centrales* located in the dorsal and ventral regions of the retina *in lieu* of a vertical streak provides the species with the adaptations for different tasks, required to address the visual field either above or below the horizon, or according to the orientation of the fish. Although the red lionfish does not coexist in the same geographic locations as most of the species in the previous examples, it does with others of

similar ecological niches. It would be valid to assume that the photoreceptor configuration in its retina suits its diverse ecological needs.

Lionfish are active predators that prefer low light environments to ambush their prey. Being voracious hunters and generalist consumers, they prey both on benthic and pelagic organisms (Pabón & Acero, 2016), and hence require different strategies to strike their prey. In addition to direct strikes, lionfish can blow directed jets of water at prey fish, both cryptobenthic and mobile (Albins & Lyons, 2012). This requires them to adopt different positions while swimming in a vertical and diagonal range, facing different angles of light penetration in the water column.

Lionfish can occupy turbid environments such as mangrove swamps or river mouths or open environments where they roam at dusk or dawn, but more cautiously during daylight hours, while staying close to reefs, crevasses or sunken ships among others solid structures that provide shade (Arbeláez & Acero, 2016; Bogdanoff, 2020; Morris, 2012). Due to turbidity levels and the high presence of underwater tree roots, mangrove swamps serve as shelter to juvenile lionfish individuals that can not only protect themselves against potential predators but also consume local species in their early life stages, therefore representing an ecologic threat (Arbeláez & Acero, 2016). Although they inhabit shallow waters during their early life stages, lionfish tend to occupy deeper waters as they become older and increase in size (Morris, 2012), which suggests their visual system needs to be adapted to survive in the dark.

The vertically predominant distribution of cones suggests, on one hand, that each region of the retina follows a specific task, such as detecting prey on the substrate (ventral) while looking for silhouettes (potential predators) above (dorsal). On the other hand, the species needs to be adapted to vertical displacement by being able to obtain as much possible information from the

remaining light as it diminishes by reaching greater depths or from variations in observable patterns, such as shadows or dark contrasts at different depth levels. Moreover, the visible area above the animal is limited by Snell's window -a patch of light that appears on the surface of water when and observer looks underwater from above, which adopts a circular shape due to refraction when light passed from air to water (Wood, 1911), while areas below become less visible due to light scattering and absorption. Because of the angle of incidence of direct light, dusk and dawn would provide the best illumination in those areas. In this context, it has been demonstrated that predatory fish utilize Snell's window to illuminate prey underwater (Janssen, 1981; Thetmeyer & Kils, 1996), which could be the case for the red lionfish. Still, it is possible that different areas of the retina featuring notoriously different photoreceptor densities also feature different spectral sensitivities, which could be addressed by investigating opsin expression across the retina.

From an anatomical perspective, species with vertically elongated pupils such as felines and reptiles (to my knowledge, this orientation does not occur in fish) are very likely to be ambush predators and active day and night, since vertical-slit pupils maximize stereopsis and blur, in which objects at different distances are out of focus (Banks et al., 2015). Most teleost feature protruding eyes to allow a certain degree of periscopic vision and circular pupillary openings sometimes irrupted by an aphakic gap (Fernald, 1988). In the absence of a vertical pupil (as seen in Figure 6), a vertically dominant distribution of photoreceptors would be a suitable adaptation for the red lionfish, being an active hunter and occupying such a wide vertical habitat range (Côté et al., 2013). The strength of this linkage between hunting efficiency and migratory patterns with photoreceptor distribution remains to be assessed through formal research.

Intraspecific and interspecific interactions are not to be discarded when discussing the significance of photoreceptor distribution. A vertical spread as the one observed in *A. akindynos* (Stieb et al., 2019) suggests an association with vertical body stripes which are essential for species recognition (Salis et al., 2018); this could be the case for the red lionfish as well as all other lionfish species, since they display vertical body stripes. Lönnstedt et al. (2014) describe how two lionfish species, *Dendrochirus zebra* and *Pterois antennata*, engage in cooperative hunting by a stereotyped flared fin display, evidencing complex collaborative foraging behaviours in lionfish. Visual body patterns such as vertical stripes are essential in these sorts of display. Then again, further field observations and behavioural tests will be needed to confirm this assumption.

4.2.2 Photoreceptor Types

I was able to recognize four different types of photoreceptors in the outer layer of the retinal surface of the red lionfish: rods, single cones, double cones and triple cones. Rods covered the entire retinal surface but were discarded from photoreceptor counts. Single and double cones also occur all over the retinal surface, especially towards the dorsal and ventral areas; they spread along the retina in a similar fashion, with a rather vertical orientation, maintaining a 2:1 to 4.5:1 double-to-single cone ratio in a square mosaic pattern. Triple cones only exist in the proximities of the optic nerve and along the falciform process. Since they occur in small numbers, I did not include them in the counting to generate retinal maps. From this point forward, it is worth outlining specific references on fish photoreceptor size, diameter and distribution are scarce -at least for public access. Therefore, performing accurate comparisons between phylogenetically related species, or even species sharing the same habitat, was not always attainable.

Lionfish prefer downwelling light environments, being able to inhabit deep-water environments down to 300 m depth (Morris, 2012). They have been reported to be crepuscular in their native range but are particularly active in daylight hours in Bahamian (Côté & Maljković, 2010) and Colombian coral reefs -as I have personally observed during scuba diving excursions (Appendix F), usually retreating to ledges and crevices among the rocks and corals as well as artificial structures. As one crucial aspect for survival of carnivore organisms in a new environment is predatory efficiency, which relies heavily on visual capabilities, scotopic (low-light) vision is beneficial for hunting success in shallow waters as lionfish prey capture rates are significantly higher in areas where direct sunlight is scarce (Côté & Maljković, 2010). This is especially relevant for younger, smaller lionfish, since they prefer shallow and/or nearshore habitats (McGuire & Hill, 2021) and are more dependent on their jet blowing ability -as it requires a more accurate visualization of prey- than larger individuals (Albins & Lyons, 2012). Taking this into account, it would be pertinent to inquire if there are differences in photoreceptor distribution and peak photoreceptor sensitivity between young and adult lionfish.

4.2.3 Square Mosaic Pattern

Spatial configuration of different types of cones in the retina of *P. volitants* feature single and double cones displaying a square mosaic pattern in regions where triple cones are absent. Mosaic patterns are featured in the retinas of most teleost fish, as described by several authors (Ali & Anctil, 1976; Brainard, 2019; Fritsch et al., 2017; Hunt et al., 2015) and can be classified as row, square and triangular mosaic patterns depending on the how cone types are located in relation to each other. The square mosaic pattern consists, as observed, in quadrilateral units of one central single cone surrounded by four double cones or else an empty (i.e., rod-dominated) space among four double cones. In the red lionfish, distance within cones were greater in some areas of the

retina than in others, corresponding to smaller cone sizes and hence to greater densities, as it is presented in retinal maps.

Square mosaic patterns have been described in several shallow-water diurnal teleosts in which survival has been proved to depend on visual capabilities (Engström, 1963; Lyall, 1957; Nag & Bhattacharjee, 1993; Nicol, 1989). This arrangement is an ideal visual adaptation to perceiving moving objects and prey, therefore facilitating predation of living fish (Hunt et al., 2015). Although uncommon in fish species, Cameron and Pugh (1991) outline that typical mosaic patterns featuring relatively larger amounts of double cones may be related to detection of polarized light, an important feature for searching and recognition of prey in turbid waters. This can provide an understanding on how lionfish are able to occupy shallow water with low levels of light penetration (e.g., turbid) or deep waters, while maintaining predatory efficiency.

4.2.4 Photoreceptor Cell Densities

Density was estimated as 3378.28 $\pm$ 1261.48 cells/mm^2 for single cones and 7612.31 $\pm$ 2143.91 cells/mm^2 for double cones. These densities are remarkably lower than the average found in the largemouth bass (*Micropterus salmoides*; SC: 10000 cells/mm^2; DC: 32000 cells/mm^2) (J. G. Kim et al., 2022) and *T. delaisi* (SC: 10200 cells/mm^2; DC: 23300 cells/mm^2) (Fritsch et al., 2017), and peak values in *A. akindynos* (SC: 178800 cells/mm^2; DC: 358800 cells/mm^2) (Stieb et al., 2019). Some bibliographic references only provide an estimated total density of single and double cones. In the red lionfish, total cone density is 10990.59 cells/mm^2, similar to Degen's leatherjacket (*Tamnaconus degeni*) and the crested flounder (*Lophonectes gallus*) with ~10000 cells/mm^2, although considerably higher than in the silver biddy (*Parequula melbournensis*: 2350 cells/mm^2), the planktivorous big eye kilka (*Clupeonella grimmi*; 2938 $\pm$ 77 cells/mm^2), the eastern school whiting (*Sillago flindersi*), the ambush predator tiger flathead (*Neoplatycephalus*

richardsoni), the sand flathead (*Platycephalus bassensis*), the roundsnout gurnard (*Lepidotrigla mulhalli*) and the planktivore Jack mackerel (*Trachurus declivis*) with 3800-6000 per mm^2) (Hunt et al., 2015; Khalili et al., 2014).

Relatively low cone densities indicate the importance of rod-dominated spaces for scotopic vision, as rods are much more sensitive to low levels of light than cones (Fernald, 1988). Rods covered every cone-free area in the retina of the red lionfish, making up for gaps of single cones in the square mosaic pattern. This provides the species the capacity to maintain scotopic sensitivity concurrently with color vision.

Higher cone densities are associated to higher visual acuity for color vision, especially in daylight (Baars & Gage, 2012; Nag & Bhattacharjee, 2002). Color vision is especially important for young fish to be able to observe and characterize environments as colorful as coral reefs. Among other advantages, it is useful to detect their prey such as small fish or zooplankton that reflects light due to its transparence, and their predators, that are usually large and conspicuous enough to be noticed from a distance (Marshall et al., 2019). The typical cone density in diurnal teleost fishes is over 40000 cells/mm^2 (Ali & Anctil, 1976; McFarland & Munz, 1975). According to this, the visual system of the red lionfish as such is not specialized for color vision. As mentioned previously, rods occur all over the retinal surface, suggesting the necessity of combining dim-light visual capabilities with color vision, along with other mechanisms such as a partially cryptic behaviour, to perform well in high-light environments.

Triple cones had an average density of 1773.33 $\pm$ 1089.99 cells/mm^2. Triple and quadruple cones are not the dominant type in nature but are rather common in teleost species. Studies on the morphology and distribution of triple cone cells date from mid-20th century but knowledge about

their size, density and adaptive functionality is still scarce. In some cases, their numbers are reported as part of a cone cluster (e.g.: triple-cone units x 3 + single cones) (Heß, 2009), making it inconvenient for comparison purposes. The only observed report on density values states *T. delaisi* presents 16700 $\pm$ 2500 triple cone cells/mm^2 (Fritsch et al., 2017), a number more than nine times greater than in the red lionfish.

Heß (2009) provides 41 reports of occurrences and distribution of triple cones across the retinal surface in teleost specie -38 by 11 other authors and three of his own. The most common location is near the optic nerve (9), followed by a more diffuse spread over the retina (7), aggregation in the dorsal area (4), centralized but often diffuse (4); they are less common as dominant all over the retinal surface, at the temporal fundus, the area dorsal to the optic nerve, central area near the optic nerve, dorso-temporal cluster, diffuse but rather abundant or frequent, diffuse and scarce, or at the fundus. Location of triple cones in the retina of the red lionfish corresponds to the dominant one in the reports above with the addition of a tendency to spread towards the ventral pole. All nine species are carnivores, but only three of them are active predators same as the red lionfish, plus none of them is phylogenetically related.

The shortage of studies on triple cones implies a void in terms of the adaptive significance of these photoreceptor cells, much less regarding the behavioural ecology of a species. In some fish species, triple cones are simply a product of regeneration processes after previous damage to the retina, hence, they are considered malformations (Cameron & Powers, 2000; Cameron & Easter, 1995). This would make sense for the red lionfish as triple cones align with the falciform process, which, as vascular structure, irrigates and provides nutrients to the retina, hence supporting regeneration processes. Nevertheless, triple cones are rather abundant, even being the dominant type of photoreceptor in most fish species, which signifies circumstantial evidence to a role in

vision. In many anchovy and minnow species, triple cones are not only abundant and larger than other cone types, but also feature unequal morphologies (i.e., at least one of the cones being smaller than the other two). It has been suggested that larger sizes denote lower densities and hence lower potential visual acuity, and that unequal cone morphology may indicate increased sensitivity in relation to other cones, serving a function of color discrimination that would provide color-blind polarization vision and support color discrimination capabilities (Collin et al., 1996; Heß, 2009; Kondrashev et al., 2012; Loukashkin & Grant, 1965). Since triple cones in the red lionfish are scarce, morphologically equal and there is no data on their spectral sensitivity, further studies would be required to support any of the previous statements to provide more accurate ones in relation to the biology of the species.

4.3 GA cells Distribution and Configuration Patterns

It is worth recalling at this point of this document that due to methodological issues, any results derived from GA cell counting (i.e., distribution maps, cell patterns, estimated densities and SRP) are based on two retinal tissue samples only, one for each eye. Among other inconveniences, I observed an overabundance and clustering of GA cells -and possibly other types of neural cells. It was not possible at this time to provide an accurate number or distribution pattern of specific neural cells, to determine if glomerulal patterns were composed only of ganglion cells or other type of cells, to attribute glomerular or other configurations to specific sections of the retina. This inevitably provides my research with a lack of accuracy, at the point to be consider results and conclusions as preliminary but worth to revise through further studies.

Nonetheless, topographic maps for GA cells showed that these are more abundant towards the ventro-nasal region of the retina and do not match the overall distribution of photoreceptors. Although there are numerous references to ganglion cell densities, distribution and ecological advantages in scientific literature, the fact that ganglion and amacrine cells are part of the same counting unit in this study would make density comparisons inaccurate; moreover, references on ganglion cell topography of phylogenetically related species to the red lionfish are absent in the existing literature.

Ganglion cell distribution for 12 species of reef teleosts (Collin & Pettigrew, 1988a, 1988b; Fritsch et al., 2017; Stieb et al., 2019) are displayed in maps suitable for comparison. More than half of them display centralized, mostly temporal to nasal, horizontal streaks; some feature a dual zone with higher cell densities, such as an *area centralis* in addition to a horizontal streak, or two *areae centrales* in either the temporal, nasal and or dorsal regions. Instead, 18 species of deep-sea lanternfishes present either concentrated temporo-ventral or simply temporal areas as a majority, and if not, a typical *area centralis* (de Busserolles et al., 2014). Horizontal streaks in reef fish are deemed a suitable adaptation for predatory surveillance or feeding behaviour when swimming in deep terraced reef fronts or areas of open water (Collin & Pettigrew, 1988b). Ventral elongated areas (e.g., ventro-temporal) will connect the frontal and dorsal visual field and even allow the perception of silhouettes when facing a more illuminated background (de Busserolles et al., 2014).

GA cells (i.e., ganglion and amacrine cells) were abundant all over the inner layer of the retinal tissue, occasionally gathered as glomeruli. Average and maximum counts were respectively of 49576.09 $\pm$ 13161.19 cells/mm^2 and 105000 cells/mm^2 considering an extremely conservative approach.

Glomerular arrangements have been described as fundamental units of brain organization in different sensory systems in some vertebrate species. In mice, olfactory bulbs contain glomerular arrays in which each glomerulus acts as an individual channel of olfactory information, as they send afferent inputs to mitral cells -a type of neuronal cell type in the olfactory bulb while surrounded by other glomeruli that act as inhibitor field and as individual emitters themselves (Fantana et al., 2008; LaMantia & Purves, 1989). In the macaque monkey retina, midget bipolar cells connect through axon terminals to midget ganglion cells that are part of foveal circuitry; these axon terminals form a glomerular structure, serving as individual connections from/to each bipolar and ganglion cell (Wool et al., 2019).

The function of glomeruli in the retina of fish species is yet to be discussed. Based on related studies in other vertebrates (Fantana et al., 2008; LaMantia & Purves, 1989; Wool et al., 2019), it would be accurate to assume a role as center-surround receptive arrangements, becoming individual channels to a certain number of photoreceptors. This would denote a different level of visual processing depending on the arrangement and overlapped distribution -if any- of GA cells and photoreceptors.

4.4 Alignments between Photoreceptor and GA Cell Distribution

As presented next, studies on retinal topography in teleosts (Champ et al., 2014; Dalton et al., 2017; Kock, 1982) demonstrate that distribution of photoreceptors are not always consistent with distribution of ganglion cells, which suggests discrepancies in topographies could be related to sectorized requirements in the visual system. In the coral reef triggerfish *Rhinecantus aculeatus*, photoreceptors display a fully horizontal streak while greater densities of ganglion cells also

spread horizontally although only partially, extending to the nasal pole and not the temporal pole (Champ et al., 2014). In the cichlid fish *Metriaclima zebra*, photoreceptor cells are more abundant towards the periphery and as a partial horizontal streak towards the temporal pole, while ganglion cells are more numerous as a fully horizontal streak; additionally, they are both concentrated as an *area centralis* near the optic nerve head (Dalton et al., 2017). Both examples imply higher behavioural acuity in areas where high photoreceptor and ganglion cell densities overlap; this, as long as convergence rations remain low, since the lower the convergence ratio, less spatial information between photoreceptor and ganglion cell layers is lost (Kock, 1982).

In the retina of the red lionfish, while photoreceptors spread vertically rather than horizontally, ganglion cells do not follow this pattern and concentrate ventro-nasally, pointing to a greater need for processing visual stimuli coming from below. This would be relevant for the species in terms of predator-prey dynamics and vertical displacement. As a general predator, the red lionfish can consume organisms dwelling on the seafloor, which would be able to pick using binocular vision as an advantage. Additionally, as growing or adult lionfish reach deeper waters, they must be able to identify any organisms that may serve as a food source, but also to be aware of any potential predators that could directly threaten their survival or signify a potential risk to juveniles growing in a novel environment.

GA cells: single-double cones ratio ranged from 3.10:1 to 4.57:1 in different areas of the retina, which would suggest some information is lost between layers. A ganglion cell-cone ratio of 1:1 or close, would indicate prioritizing of acuity (i.e., resolution) over sensitivity, as it is the case of *T delaisi* (Fritsch et al., 2017). In other fish species, a higher summation ratio of ganglion cells to photoreceptors provides greater sensitivity, while a lower ratio corresponds to enhanced resolution (Garza-Gisholt et al., 2018). My results would suggest greater sensitivity over

resolution. Nevertheless, as indicated in the previous section, counting ganglion and amacrine cells altogether will inevitably increase numbers and ratios. For a more accurate assessment on this aspect of this study, that is, an accurate estimation of ganglion cell population to generate assumptions in relation to visual acuity and sensitivity, it would be imperative to distinguish ganglion cells from amacrine and other neural cells.

4.5 Spatial Resolving Power

Spatial resolving power in the red lionfish had a range of 7.97-18.42 cpd for photoreceptors and 10.69-30.99 cpd for GA cells. Previous studies have provided SRP values by means of either photoreceptor or retinal ganglion cell densities, as it is, statistically speaking, equally valid and even comparable for analyses (Caves et al., 2017). Visual acuity (i.e., spatial resolving power) can be estimated anatomically by measuring cell density and intercellular spacing in the retinal surface, hence providing quantifiable data of the information that is available to a certain species in a certain environment (Caves et al., 2018; Cronin et al., 2014). Behavioural estimations, on the other hand, determine how a species can interact with its environment given the information available, related to post-retinal processing rather than optical capabilities (Caves et al., 2018; Cronin et al., 2014). These two estimates are comparable, not in an aspect of accuracy or reliability, but rather being complementary, as they provide a deeper insight on the influence of both anatomical and neural processing in a species to perceive and adapt to its environment (Caves et al., 2021).

Anatomical estimation of acuity by means of ganglion cell densities should signify a more accurate estimate than with photoreceptors (Wagner, 1990). Ganglion cells are located further in

the visual processing pathway than photoreceptors and hence perform a major role when it comes to provide visual acuity to vertebrates (Devries & Baylor, 1997; Enroth-Cugell & Robson, 1966; Lee & Stevens, 2007; Pettigrew et al., 1988). Estimating SRP by combining ganglion and amacrine cells may result in an overestimation (de Busserolles et al., 2014), and values obtained by ganglion cell density only would provide values closer to reality. Moreover, an accurate estimation of SRP that includes retinal ganglion cells only allows determining two different values for opposite purposes. In the range of SRP values, the lower and higher values relate to color vision and rods respectively, indicating approximate spatial resolution values for photopic (day) and scotopic vision (McFarland & Munz, 1975). Temporal adaptations to day or night conditions also depend on the divergence in the ON and OFF pathways led by bipolar and ganglion cells for visual processing (Pandarinath et al., 2010). Thus, a species such as the lionfish should perform better in terms of spatial resolution when relying on scotopic vision rather than photopic, a hypothesis that requires further examination.

With this in mind, considering the fact that the estimated densities for ganglion cells in this study also include amacrine cells (therefore named GA cells) and the obtained values are considerably high for fish species, I addressed only the estimated SRP range of 7.97-18.42 cpd obtained for photoreceptors. SRP for the red lionfish falls into a rather intermediate to high range of values among reef teleosts (4-27 cpd) and deep-sea teleosts (1.3-22.9 cpd) (Collin et al., 1997; Collin & Partridge, 1996; Wagner et al., 1998). While a greater SRP relates with a more active and high-visual-acuity-dependent feeding strategy, lower values usually indicate a greater need for visual sensitivity rather than acuity, as well as the use of other sensory systems (Bailes et al., 2006; Collin & Pettigrew, 1989; de Busserolles et al., 2014; Wagner, 1990).

Fish species that tend to switch between environments frequently, migrate horizontally, or vertically, during different life stages require higher resolving power than those that remain in the same one, as they contend with fluctuating visual conditions in terms of light penetration and overall visibility (Caves et al., 2017). My findings suggest the red lionfish shares the visual adaptability of active predator reef teleosts, which will be better explained through a more thorough description of the visual system based on photoreceptor and GA cell morphology and retinal topography. Nevertheless, considering the ecology of the red lionfish, additional adaptations for dim-light environments such as the presence of a *stratum argenteum* should not be discarded.

4.6 Photoreceptor Size

Single cones had an average diameter of 3.36 ± 0.50 μm. Their size is much smaller to other marine predatory fish such as *P. bassensis* (5.0 ± 0.6 μm), *L. gallus* (6.0 ± 0.0 μm), *L. mulhalli* (6.0 ± 1.1 μm), *S. flindersi* (11.0 ± 0.7 μm), and freshwater predatory fish such as the aucha perch (*Coreperca herzi*; 6.6 ± 0.5 μm) (Hunt et al., 2015; Kim et al., 2014, 2022). Some marine and freshwater fish instead feature similarly small single cone diameters, as it is the case of *P. melbournensis* (4.0 ± 0.5 μm), *T. degeni* (2.0 ± 0.5 μm), *M. salmoides* (3.8 ± 0.2 μm) and the bluegill (*Lepomis macrochirus*; 3.3 ± 0.3 μm) (Hunt et al., 2015; Kim et al., 2014, 2022).

Double cones had an average length and width of 6.95 ± 0.48 μm and 3.46 ± 0.43 μm. For size comparison purposes, I only considered their length. Double cone diameter is consistently smaller than in marine predatory fish *L. gallus* (11.0 ± 1.5 μm), T. degeni (8.0 ± 0.5 μm), *P. melbournensis* (8.0 ± 0.6 μm), *P. bassensis* (12.0 ± 1.2 μm), *S. flindersi* (16.0 ± 0.8 μm), *L.*

mulhalli (16.0 ± 0.9 μm), and freshwater predatory fish *L. macrochirus* (7.5 ± 0.4 μm), *M. salmoides* (7.5 ± 0.2 μm) and *C. herzi* (11.3 ± 0.4 μm) (Hunt et al., 2015; Kim et al., 2014, 2022).

Triple cones had an average diameter of 6.73 ± 0.67 μm. They are smaller than triple cones in the white hake (*Urophycis tenuis*) and the American pollock (*Pollachius virens*) with 10 μm each, the anchovies *Cetengraulis mysticetus* (15 μm), *Engraulis encrasicolus* 16 μm, *Anchovia macrolepidota* (18 μm) and the yellowtail (*Limanda ferruginae*) with 18 μm (Collins & MacNichol, 1979; Heß, 2009). In some of these species, triple cones are rather oval shaped with a small cone imbedded into two large ones.

A small diameter of an object in a given space is directly related to larger numbers -the smaller the diameter of cones, the higher density of visual cells (Tamura & Wisby, 1963). Density, along with arrangement and diversity of cone cells, may induce to a higher visual acuity in an organism, therefore enhancing movement recognition (Kim et al., 2014; Salem, 2016) and even a rapid visual response to prey recognition when there is an overwhelming presence of rod cells (Kim et al., 2022).

In the case of the red lionfish, even though smaller photoreceptor size allows a smaller increase in numbers, rods are abundant in areas not occupied by cones. While the presence of cones and the square pattern displayed indicates the capacity for color vision, rod dominance suggests a trade-off between photopic and scotopic vision considering the species' ecology, could provide an advantage when establishing a feeding ground in a novel habitat. According to Salem (2016) in his work on the round sardinella (*Sardinella aurita*), a higher visual acuity can also facilitate long-distance swimming, which is also beneficial for the red lionfish not in terms of migration – since, as indicated earlier, it is not a migratory species-, but rather in terms of invasive potential.

This, in addition to broad environmental tolerances, high reproductive output, defense from predation, and a generalist feeding strategy, the main factors contributing to the rapid expansion and establishment of lionfish (Côté et al., 2013).

4.7 Research Gaps and Potential Insight

This research focused on the determination of different types of photoreceptor and neural cells present in the retina of the red lionfish, allowing the generation of maps to display the distribution of certain visual cell along the retinal surface in a way to provide a better understanding of the species' ecology based on visual capabilities. Nevertheless, due to methodological impasses, lack of available information and other common issues in scientific research projects of this sort, there are still voids of information that could eventually provide further knowledge on the visual ecology of the red lionfish and other teleost species.

First off, including rods in photoreceptor counts will be an important contribution in the evaluation of scotopic sensitivity of the species, which, as mentioned before, is a key aspect of its ecology. It is also worth mentioning the possibility of a multibank retina (i.e. one layer of cones over several layers of rods) in the red lionfish, as multibank retinas are common in teleost species that inhabit dim-light environments, including deep-sea, nocturnal shallow or freshwater species, but their specific function and structural characteristics remains unresolved (de Busserolles et al., 2020). Special arrangements of retinal cells such as a multibank retina can only be determined by generating cross sections through basic histological procedures.

Still regarding photoreceptors, determining opsin expression can provide a measure of light absorption, which, ideally, would correspond to the different densities estimated in different

regions of the retinal surface and represented in the topographic maps (Cortesi et al., 2020; Luehrmann et al., 2018).

Possibly the greatest limitation in this study was the number of samples used for GA cell counting, as they were only two (one right eye, one left eye). As mentioned previously, there were some difficulties during the dissection process and the disassembling and flipping of photoreceptor wholemounts for GA cell counting because of which some retinal tissue suffered damage and became unsuitable for wholemounting. For logistic reasons, obtaining new samples was out of question at the time.

Moreover, establishing an accurate differentiation between ganglion cells and other neural cells will be highly relevant to observe a proper configuration of glomeruli (e.g., to determine if they are composed of ganglion cells only) and their distribution across the retinal surface. This would lead to a more thorough revision of sectorized requirements of the visual system on both the inner and outer retinal surface. In this same context, a proper identification of retinal ganglion cells would have been ideal for the estimation of SRP, as it has been mentioned, these values are closer to reality, to obtaining photopic and scotopic limits for visual acuity, and even to perform statistical comparisons between photoreceptor- and ganglion cells-obtained values. Due to the limitations concerning visual identification and counting of retinal photoreceptor and neural cells, greater accuracy in cell visualization should be performed by means of more sophisticated magnification procedures such as electron microscopy, in conjunction with imaging software for measuring and counting as the one used in this project.

SRP features also relate to photoreceptor distribution patterns, such as the square mosaic found in this study, since the distance between cone centers in specific packings can translate to a certain

range of degrees of visual angle. Calculating average distance between photoreceptors in low and high-density areas should help obtaining differences in spatial resolution in different regions of the retinal, in relation to the sectorized requirements. Photoreceptor types, patterns, distribution, peak sensitivity and other mentioned parameters should certainly be determined in young and adult lionfish for comparison purposes.

There is an additional limitation related to the size of the fish used in this study. With an average fully matured adult size of ≤ 35 cm Total Length, male red lionfishes reach sexual maturity at 10 cm while females at 18 cm (Gardner et al., 2015). The specimens from which my final samples were obtained ranged from 12.90 to 16.90 cm Standard Length. Red lionfish do not feature a notorious sexual dimorphism, plus I did not assess their sexual maturity based on gonadal development, making it impossible to determine if these individuals were fully matured males, immature females, or a mixture of both. An unclear differentiation between males and females and levels of sexual maturity among individuals was an impediment for me to determining if photoreceptor and/or GA cell distribution and patterns differ between juveniles and adult fish. If this was the case, the retinal maps between these two groups would look substantially different and therefore represent different adaptative advantages that should be addressed in accordance with their ecology, the environments they occupy and their feeding habits, among other aspects. In this context, there would also be differences in the SPR and peak sensitivity between young and adult fish.

Lastly, the shortage of information in reference to comparable species, either phylogenetically related or occupying a similar niche, was another limiting factor. For that matter, a compilation of topographic maps of retinal cell distribution in vertebrates (Collin, 2008) remains inaccessible at this time.

4.8 Research Opportunities towards Understanding the Visual System and Ecology of the Red Lionfish

Studying the visual system of any organism provides a considerable amount of information that can be used to understanding the way it perceives its environment and the diversity of behaviours it can adopt according to visual stimuli. Environmental information that can be obtained from the remaining light while reaching greater depths, as well as prey detection, predator-prey interactions, mate recognition, kin recognition and other species-specific social interaction directly related to visual perception have been discussed throughout this document. This does not limit the extent of the applicability of the knowledge hereby acquired.

A histology approach, as a visual depiction of longitudinal sections of the retina composed of layers conforming the visual processing pathway from photoreceptors to ganglion cells, would be an ideal starting point to visualizing the overall structure of the retina.

As discussed previously, a vertical dominance of photoreceptors in the red lionfish relates to the wide vertical spatial range the species occupies and possibly to the vertical stripes on its body. Any related hypothesis needs assessment by field observations and/or behavioural tests.

As an additional visual aspect, SRP can be estimated measuring the contrast sensitivity as a function of different spatial frequencies (Santon et al., 2019). Studies addressed to this feature would contribute to the understanding of the visual capabilities of the red lionfish.

On a separate note, although as it has been mentioned in this document, *Pterois volitans* is a highly invasive species, what seems to be a common feature to most *Pterois* species. Even though originally from the Indo-Pacific Ocean, the red lionfish now dwells shallow and coastal waters from tropical to temperate regions of the planet. A holistic conservation approach to every

ecosystem affected by the presence of the red lionfish would then require mitigation control strategies. One key aspect to the success of the red lionfish as an invasive species is its capacity to adapt to different habitats in relation to its predation efficiency –widely benefited by its visual capabilities. Understanding how a top predator perceives its environment is by all means relevant to be able to lure and hunt its prey.

While lionfish are solitary predators, they tend to adopt an aggregation behaviour, which seems to be coincidentally based on individuals' mutual attraction to similar reef structure, to maximize hunting efficiency (Hunt, et al., 2019). Some species of lionfish even engage in cooperative hunting by means of flared displays to coordinate and take turns striking at their prey (Lönnstedt et al., 2014). Lionfish aggregation devices (LADs) have been implemented in different areas of the Caribbean Sea and North Atlantic Ocean to induce lionfish group formation and encourage their capture by scuba divers (Bogdanoff, 2020). In this regard, the sort of bait juveniles or young fish that are still found in shallow waters are mostly attracted to, in a way to remove them from the area before they reach a sexual maturity age, hence preventing further reproduction.

A study by Blackmore et al. (2022) on the use of LED lights on cod line fishing to reduce bycatch -hence improving fishing efficiency, could be the starting point to applying similar technologies (i.e., specific light stimuli) to lure lionfish in areas where fishing or poaching is encouraged, or to devices such as LADs as the ones mentioned above.

So far, this research has provided an initial insight on visual capabilities and subsequent ecological implications in the red lionfish. There are, though, further aspects to explore on the path to acquire a more holistic understanding of the visual ecology of this or any other organism.

The previous examples are merely a glimpse of the potential that currently exists in the fields of visual and behavioural ecology.

5. CONCLUSION

In this project, was able to identify rods and cones as photoreceptor cells, and ganglion and amacrine cells altogether (GA cells) as neural cells in the retina of the red lionfish *Pterois volitans*. I estimated cell densities, cell distribution patterns, and spatial resolving power for cones and GA cells. Providing this, I produced retinal maps of photoreceptor and GA cells corresponding to opposite sides of the retinal, I determined alignments between cell distribution, I established single-to-double cone and GA-cone ratio, identified cell patterns and estimated spatial resolving power. My results and observations along with bibliographical insight of the ecology and behaviour of the red lionfish allowed me to discuss certain relationships between visual and behavioural adaptations in the species.

Similar to what I hypothesized, photoreceptors are more dominant in a vertical axis, as two *areae centrales* in lieu of a vertical streak. This suggests an advantage to the species in terms of roaming during dim-light moments of the day or inhabiting downwelling light environments, such as areas of low light penetration due to turbidity levels or greater depths. On a similar note, not only spatial distribution of photoreceptor and GA cells in the retinal surface but also photoreceptor configuration in a square mosaic pattern address my speculations over spatial orientation and clarity of image. A visual system with these adaptations is key to the red lionfish jet squirting ability, as well as to track and strike its prey efficiently in different vertical body positions and light environments in accordance with light penetration levels.

I accordance to my results and assumptions, the red lionfish is highly capable of occupying and detecting potential prey in environments with different levels of light penetration. These two factors are key to the species invasive capabilities in addition to the aforementioned high salinity tolerance, high fecundity, larval survival rate and colonizing persistence. My findings should still be supported by field observations and behavioural experiments.

6. REFERENCES

Albins, M., & Lyons, P. (2012). Invasive red lionfish *Pterois volitans* blow directed jets of water at prey fish. *Marine Ecology Progress Series*, *448*, 1–5. https://doi.org/10.3354/meps09580

Ali, M.-A., & Anctil, M. (1976). Retinas of fishes. Springer Berlin, Heidelberg. https://doi.org/10.1007/978-3-642-66435-9

Applegate, R. A., Marsack, J. D., Ramos, R., & Sarver, E. J. (2003). Interaction between aberrations to improve or reduce visual performance. Journal of Cataract and Refractive Surgery, 29(8), 1487–1495. https://doi.org/10.1016/s0886-3350(03)00334-1

Arbeláez M., N., & Acero P., A. (2016). Presencia del pez león *Pterois volitans* (Linnaeus) en el manglar de la bahía de Chengue, caribe colombiano. Bulletin of Marine and Coastal Research, 40(2). https://doi.org/10.25268/bimc.invemar.2011.40.2.123

Baars, B., & Gage, N. M. (2012). Fundamentals of cognitive neuroscience: A beginner's guide. Academic Press.

Bailes, H. J., Robinson, S. R., Trezise, A. E. O., & Collin, S. P. (2006). Morphology, characterization and distribution of retinal photoreceptors in the Australian lungfish *Neoceratodus forsteri* (Krefft , 1870). The Journal of Comparative Neurology, *494*, 381–397.

Banks, M. S., Sprague, W. W., Schmoll, J., Parnell, J. A. Q., & Love, G. D. (2015). Why do animal eyes have pupils of different shapes? Science Advances, 1(7), e1500391. https://doi.org/10.1126/sciadv.1500391

Blackmore, R., Winger, P., Bitton, P.-P., Bayse, S., Whittaker, K., & Montevecchi, W. (2022). The effects of LED handline attachments on Atlantic cod (*Gadus morhua*) catch efficacy and bycatch. Fisheries Research, 258, 106543. https://doi.org/10.1016/j.fishres.2022.106543

Bogdanoff, A. K. (2020). Management of invasive lionfish (*Pterois* spp.) in the temperate and tropical Western Atlantic. https://doi.org/10.13140/RG.2.2.35922.71368

Brainard, D. H. (2019). Color, pattern, and the retinal cone mosaic. Current Opinion in Behavioral Sciences, 30, 41–47. https://doi.org/10.1016/j.cobeha.2019.05.005

Cameron, D. A., & Powers, M. K. (2000). Morphology and visual pigment content of photoreceptors from injured goldfish retina. Visual Neuroscience, 17(4), 623–630. https://doi.org/10.1017/s0952523800174115

Cameron, D. A., & Pugh, E. N. (1991). Double cones as a basis for a new type of polarization vision in vertebrates. Nature, 353(6340), Article 6340. https://doi.org/10.1038/353161a0

Cameron, D., & Easter, S. (1995). Cone photoreceptor regeneration in adult fish retina: Phenotypic determination and mosaic pattern formation. The Journal of Neuroscience, 15(3), 2255–2271. https://doi.org/10.1523/JNEUROSCI.15-03-02255.1995

Carleton, K. L., Escobar-Camacho, D., Stieb, S. M., Cortesi, F., & Marshall, N. J. (2020). Seeing the rainbow: Mechanisms underlying spectral sensitivity in teleost fishes. Journal of Experimental Biology, 223(8), jeb193334. https://doi.org/10.1242/jeb.193334

Caves, E. M., Brandley, N. C., & Johnsen, S. (2018). Visual acuity and the evolution of signals. Trends in Ecology & Evolution, 33(5), 358–372. https://doi.org/10.1016/j.tree.2018.03.001

Caves, E. M., de Busserolles, F., & Kelley, L. A. (2021). Sex differences in behavioural and anatomical estimates of visual acuity in the green swordtail, *Xiphophorus helleri*. Journal of Experimental Biology, 224(24), jeb243420. https://doi.org/10.1242/jeb.243420

Caves, E. M., Sutton, T. T., & Johnsen, S. (2017). Visual acuity in ray-finned fishes correlates with eye size and habitat. Journal of Experimental Biology, 220(9), 1586–1596. https://doi.org/10.1242/jeb.151183

Champ, C., Wallis, G., Vorobyev, M., Siebeck, U., & Marshall, J. (2014). Visual acuity in a species of coral reef fish: *Rhinecanthus aculeatus*. Brain, Behavior and Evolution, *83*(1), 31–42. https://doi.org/10.1159/000356977

Chevalier-Monteagudo, P., Gutiérrez, E., Ibarzábal, D., Romero, S., Isla, V., Calderín, J., & Hernández, E. (2008). Primer registro de *Pterois volitans* (Pisces: Scorpaenidae) para aguas cubanas. Solenodon, *7*, 37–40.

Cohn, B. A., Collin, S. P., Wainwright, P. C., & Schmitz, L. (2015). Retinal topography maps in R: New tools for the analysis and visualization of spatial retinal data. Journal of Vision, 15(9), 19. https://doi.org/10.1167/15.9.19

Collin, S., Collin, H., & Ali, M. A. (1996). Ultrastructure and organization of the retina and pigment epithelium in the cutlips minnow, *Exoglossum maxillingua* (Cyprinidae, Teleostei). Histology and Histopathology. https://www.semanticscholar.org/paper/Ultrastructure-and-organisation-of-the-retina-and-Collin-Collin/2223d726df01b73cc167f246e9c650e3f0669f11

Collin, S. P. (1999). Behavioural ecology and retinal cell topography. In S. N. Archer, M. B. A. Djamgoz, E. R. Loew, J. C. Partridge, & S. Vallerga (Eds.), Adaptive Mechanisms in the

Ecology of Vision (pp. 509–535). Springer Netherlands. https://doi.org/10.1007/978-94-017-0619-3_17

Collin, S. P. (2008). A web-based archive for topographic maps of retinal cell distribution in vertebrates. Clinical and Experimental Optometry, 91(1), 85–95. https://doi.org/10.1111/j.1444-0938.2007.00228.x

Collin, S. P., Hoskins, R. V., & Partridge, J. C. (1997). Tubular eyes of deep-sea fishes: A comparative study of retinal topography. Brain, Behavior and Evolution, 50(6), 335–357. https://doi.org/10.1159/000113345

Collin, S. P., & Marshall, N. (2003). Sensory processing in aquatic environments. 355. Springer New York, NY. https://doi.org/10.1007/b97656

Collin, S. P., & Partridge, J. C. (1996). Retinal specializations in the eyes of deep-sea teleosts. Journal of Fish Biology, 49(sA), 157–174. https://doi.org/10.1111/j.1095-8649.1996.tb06073.x

Collin, S. P., & Pettigrew, J. D. (1988a). Retinal topography in reef teleosts. I. Some species with well-developed areae but poorly-developed streaks. Brain, Behavior and Evolution, 31(5). https://doi.org/10.1159/000116594

Collin, S. P., & Pettigrew, J. D. (1988b). Retinal topography in reef teleosts II. Some species with prominent horizontal streaks and high-density areae. Brain Behav. Evol, 32, 13.

Collin, S. P., & Pettigrew, J. D. (1989). Quantitative comparison of the limits on visual spatial resolution set by the ganglion cell layer in twelve species of reef teleosts. Brain, Behavior and Evolution, 34(3), 184–192. https://doi.org/10.1159/000116504

Collin, S., & Shand, J. (2003). Retinal sampling and the visual field in fishes. In: Collin, S.P., Marshall, N.J. (eds) Sensory Processing in Aquatic Environments. Springer, New York, NY. https://doi.org/10.1007/978-0-387-22628-6_8

Collins, B. A., & MacNichol, E. F. (1979). Triple cones found in retinas of 3 fish species. Experientia, 35(1), 106–108. https://doi.org/10.1007/BF01917906

Cortesi, F., Mitchell, L. J., Tettamanti, V., Fogg, L. G., de Busserolles, F., Cheney, K. L., & Marshall, N. J. (2020). Visual system diversity in coral reef fishes. Seminars in Cell & Developmental Biology, 106, 31–42. https://doi.org/10.1016/j.semcdb.2020.06.007

Côté, I. M., Green, S. J., & Hixon, M. A. (2013). Predatory fish invaders: Insights from Indo-Pacific lionfish in the western Atlantic and Caribbean. Biological Conservation, 164, 50–61. https://doi.org/10.1016/j.biocon.2013.04.014

Côté, I., & Maljković, A. (2010). Predation rates of Indo-Pacific lionfish on Bahamian coral reefs. Marine Ecology Progress Series, 404. https://doi.org/10.3354/meps08458

Cronin, T. W., Johnsen, S., Marshall, N. J., & Warrant, E. J. (2014). Visual Ecology. Princeton University Press. https://press.princeton.edu/books/hardcover/9780691151847/visual-ecology

Dalton, B. E., de Busserolles, F., Marshall, N. J., & Carleton, K. L. (2017). Retinal specialization through spatially varying cell densities and opsin coexpression in cichlid fish. The Journal of Experimental Biology, *220*(Pt 2), 266–277. https://doi.org/10.1242/jeb.149211

de Busserolles, F., Cortesi, F., Fogg, L., Stieb, S. M., Luerhmann, M., & Marshall, N. J. (2020). The visual ecology of Holocentridae, a nocturnal coral reef fish family with a deep-sea-like multibank retina [Preprint]. Neuroscience. https://doi.org/10.1101/2020.05.24.113811

de Busserolles, F., Fogg, L., Cortesi, F., & Marshall, J. (2020). The exceptional diversity of visual adaptations in deep-sea teleost fishes. Seminars in Cell & Developmental Biology, 106, 20–30. https://doi.org/10.1016/j.semcdb.2020.05.027

de Busserolles, F., & Marshall, N. J. (2017). Seeing in the deep-sea: Visual adaptations in lanternfishes. Philosophical Transactions of the Royal Society B: Biological Sciences, 372(1717), 20160070. https://doi.org/10.1098/rstb.2016.0070

de Busserolles, F., Marshall, N. J., & Collin, S. P. (2014). Retinal Ganglion Cell Distribution and Spatial Resolving Power in Deep-Sea Lanternfishes (Myctophidae). Brain, Behavior and Evolution, 84(4), 262–276. https://doi.org/10.1159/000365960

Devries, S. H., & Baylor, D. A. (1997). Mosaic arrangement of ganglion cell receptive fields in rabbit retina. Journal of Neurophysiology, 78(4). https://doi.org/10.1152/jn.1997.78.4.2048

Douglas, R., & Djamgoz, M. (Eds.). (1990). The visual system of fish. Springer Netherlands. https://doi.org/10.1007/978-94-009-0411-8

Dowling, J. E. (2002). Retina. In V. S. Ramachandran (Ed.), Encyclopedia of the human brain (pp. 217–235). Academic Press. https://doi.org/10.1016/B0-12-227210-2/00303-4

Engström, K. (1963). Cone Types and Cone Arrangements in Teleost Retinae1. Acta Zoologica, 44(1–2), 179–243. https://doi.org/10.1111/j.1463-6395.1963.tb00408.x

Enroth-Cugell, C., & Robson, J. G. (1966). The contrast sensitivity of retinal ganglion cells of the cat. The Journal of Physiology, 187(3), 517–552. https://doi.org/10.1113/jphysiol.1966.sp008107

Fantana, A. L., Soucy, E. R., & Meister, M. (2008). Rat olfactory bulb mitral cells receive sparse glomerular inputs. Neuron, 59(5), 802–814. https://doi.org/10.1016/j.neuron.2008.07.039

Fernald, R. D. (1988). Aquatic adaptations in fish eyes. In J. Atema, R. R. Fay, A. N. Popper, & W. N. Tavolga (Eds.), Sensory Biology of Aquatic Animals (pp. 435–466). Springer New York. https://doi.org/10.1007/978-1-4612-3714-3_18

Freshwater, D., Hines, A., Parham, S., Wilbur, A., Sabaoun, M., Woodhead, J., Akins, J., Purdy, B., & Whitfield, P. (2009). Mitochondrial control region sequence analyses indicate dispersal from the US East Coast as the source of the invasive Indo-Pacific lionfish *Pterois volitans* in the Bahamas. Marine Biology, *156*, 1213–1221. https://doi.org/10.1007/s00227-009-1163-8

Fritsch, R., Collin, S. P., & Michiels, N. K. (2017). Anatomical analysis of the retinal specializations to a crypto-benthic, micro-predatory lifestyle in the mediterranean triplefin blenny *Tripterygion delaisi*. Frontiers in Neuroanatomy, 11, 122. https://doi.org/10.3389/fnana.2017.00122

Gardner, P. G., Frazer, T. K., Jacoby, C. A., & Yanong, R. P. E. (2015). Reproductive biology of invasive lionfish (*Pterois* spp.). Frontiers in Marine Science, 2. https://www.frontiersin.org/articles/10.3389/fmars.2015.00007

Garza-Gisholt, E., Hart, N. S., & Collin, S. P. (2018). Retinal morphology and visual specializations in three species of chimaeras, the deep-sea *R. pacifica* and *C. lignaria*, and the vertical migrator *C. milii* (Holocephali). Brain, Behavior and Evolution, 92(1–2), 47–62. https://doi.org/10.1159/000490655

Goatley, C. H. R., & Brandl, S. J. (2017). Cryptobenthic reef fishes. Current Biology, 27(11), R452–R454. https://doi.org/10.1016/j.cub.2017.03.051

González, J., Grijalba-Bendeck, M., Acero, A., & Betancur-R., R. (2009). The invasive red lionfish, Pterois volitans (Linnaeus 1758), in the southwestern Caribbean Sea. Aquatic Invasions, 4(3), 507–510. https://doi.org/10.3391/ai.2009.4.3.12

Goudie, J. (2019). The first retinal map for the black scorpionfish, *Scorpaena porcus*. Memorial University of Newfoundland.

Gress, E., Andradi-Brown, D. A., Woodall, L., Schofield, P. J., Stanley, K., & Rogers, A. D. (2017). Lionfish (*Pterois* spp.) invade the upper-bathyal zone in the western Atlantic. PeerJ, 5, e3683. https://doi.org/10.7717/peerj.3683

Guerrero, K., & Franco, Á. (2008). First record of the Indo-Pacific red lionfish *Pterois volitans* (Linnaeus, 1758) for the Dominican Republic. Aquatic Invasions, 3. https://doi.org/10.3391/ai.2008.3.2.21

Halstead, B. W., Chitwood, M. J., & Modglin, F. R. (1955). The anatomy of the venom apparatus of the zebrafish, *Pterois volitans* (Linnaeus). The Anatomical Record, 122(3), 317–333. https://doi.org/10.1002/ar.1091220304

Hernández-Abello, J. M., García Urueña, R. D. P., & Acero P, A. (2014). Estructura de tallas y preferencia al sustrato del pez león (*Pterois volitans*) (Scorpaeniformes: Scorpaenidae) en Santa Marta (Colombia). Acta Biológica Colombiana, 20(2). https://doi.org/10.15446/abc.v20n2.41611

Heß, M. (2009). Triple cones in the retinae of three anchovy species: *Engraulis encrasicolus*, *Cetengraulis mysticetus* and *Anchovia macrolepidota* (Engraulididae, Teleostei). Vision Research, 49(12), 1569–1582. https://doi.org/10.1016/j.visres.2009.03.016

Hughes, A. (1977). The topography of vision in mammals of contrasting lifestyle: comparative optics and retinal organisation. In F. Crescitelli, C. A. Dvorak, D. J. Eder, A. M. Granda, D. Hamasaki, K. Holmberg, A. Hughes, N. A. Locket, W. N. McFarland, D. B. Meyer, W. R. A. Muntz, F. W. Munz, E. C. Olson, R. W. Reyer, & F. Crescitelli (Eds.), The Visual System in Vertebrates (pp. 613–756). Springer. https://doi.org/10.1007/978-3-642-66468-7_11

Hunt, D. E., Rawlinson, N. J. F., Thomas, G. A., & Cobcroft, J. M. (2015). Investigating photoreceptor densities, potential visual acuity, and cone mosaics of shallow water, temperate fish species. Vision Research, 111, 13–21. https://doi.org/10.1016/j.visres.2015.03.017

Janssen, J. (1981). Searching for zooplankton just outside Snell's window. Limnology and Oceanography, 26(6), 1168–1171. https://doi.org/10.4319/lo.1981.26.6.1168

Jud, Z. R., Nichols, P. K., & Layman, C. A. (2015). Broad salinity tolerance in the invasive lionfish Pterois spp. May facilitate estuarine colonization. Environmental Biology of Fishes, 98(1), 135–143. https://doi.org/10.1007/s10641-014-0242-y

Khalili, H., Shabanipour, N., & Pournajafizadeh, F. (2014). Structure and arrangement of photoreceptors in the retina of big eye kilka, *Clupeonella grimmi* (Kessler 1877). 10.

Kim, J. G., Kim, S. H., Park, J. Y., & Yoo, S.-H. (2022). Correlation between feeding behaviors and retinal photoreceptor cells of largemouth bass, *Micropterus salmoides*, in Korea. Fishes, 7(1), Article 1. https://doi.org/10.3390/fishes7010025

Kim, J. G., Park, J. Y., & Kim, C. H. (2014). Visual cells in the retina of the aucha perch *Coreoperca herzi* Herzenstein, 1896 (Pisces; Centropomidae) of Korea. Journal of Applied Ichthyology, 30(1), 172–174. https://doi.org/10.1111/jai.12311

Kim, M., Eom, Y., Song, J. S., & Kim, H. M. (2018). Effect of cataract grade according to wide-field fundus images on measurement of macular thickness in cataract patients. Korean Journal of Ophthalmology : KJO, 32(3), 172–181. https://doi.org/10.3341/kjo.2017.0067

Kletou, D., Hall-Spencer, J. M., & Kleitou, P. (2016). A lionfish (*Pterois miles*) invasion has begun in the Mediterranean Sea. Marine Biodiversity Records, 9(1), 46. https://doi.org/10.1186/s41200-016-0065-y

Kock, J. H. (1982). Neuronal addition and retinal expansion during growth of the crucian carp eye. The Journal of Comparative Neurology, 209(3), 264–274. https://doi.org/10.1002/cne.902090305

Kondrashev, S. L., Miyazaki, T., Lamash, N. E., & Tsuchiya, T. (2012). Three cone opsin genes determine the properties of the visual spectra in the Japanese anchovy *Engraulis japonicus* (Engraulidae, Teleostei). Journal of Experimental Biology, jeb.078980. https://doi.org/10.1242/jeb.078980

LaMantia, A. S., & Purves, D. (1989). Development of glomerular pattern visualized in the olfactory bulbs of living mice. Nature, 341(6243), 646–649. https://doi.org/10.1038/341646a0

Lamb, T. D. (2013). Evolution of phototransduction, vertebrate photoreceptors and retina. Progress in Retinal and Eye Research, 36, 52–119. https://doi.org/10.1016/j.preteyeres.2013.06.001

Land, M. F., & Nilsson, D.-E. (2012). Animal Eyes (2nd ed.). Oxford University Press.

Lasso, C. A., Sánchez Duarte, P., Gil, D. L., & Gutiérrez, F. de P. (2010). Análisis de riesgo para especies acuáticas continentales y marinas. Instituto de Investigación de Recursos Biológicos Alexander von Humboldt. https://repository.agrosavia.co/handle/20.500.12324/13042

Lee, S., & Stevens, C. F. (2007). General design principle for scalable neural circuits in a vertebrate retina. Proceedings of the National Academy of Sciences, 104(31), 12931–12935. https://doi.org/10.1073/pnas.0705469104

Levine, M. W., & Shefner, J. M. (1981). Fundamentals of sensation and perception. Addison-Wesley Publishing Company.

Lisney, T. J., Iwaniuk, A. N., Bandet, M. V., & Wylie, D. R. (2012). Eye shape and retinal topography in owls (Aves: Strigiformes). Brain, Behavior and Evolution, 79(4), 218–236. https://doi.org/10.1159/000337760

Lisney, T. J., Potier, S., Isard, P.-F., Mentek, M., Mitkus, M., & Collin, S. P. (2020). Retinal topography in two species of flamingo (Phoenicopteriformes: Phoenicopteridae). Journal of Comparative Neurology, 528(17), 2848–2863. https://doi.org/10.1002/cne.24902

Lisney, T. J., Wylie, D. R., Kolominsky, J., & Iwaniuk, A. N. (2015). Eye Morphology and Retinal Topography in Hummingbirds (Trochilidae: Aves). brain, behavior and evolution, 86(3–4), 176–190. https://doi.org/10.1159/000441834

Lönnstedt, O. M., Ferrari, M. C. O., & Chivers, D. P. (2014). Lionfish predators use flared fin displays to initiate cooperative hunting. Biology Letters, 10(6), 20140281. https://doi.org/10.1098/rsbl.2014.0281

Loukashkin, A. S., & Grant, N. (1965). Behaviour and natural reactions of the northern anchovy, *Engraulis mordax* Girard, under the influence of light of different wave lengths and intensities and total darkness. Proceedings of the Californian Academy of Sciences, 31(24), 631–692.

Luehrmann, M., Stieb, S. M., Carleton, K. L., Pietzker, A., Cheney, K. L., & Marshall, N. J. (2018). Short-term colour vision plasticity on the reef: Changes in opsin expression under varying light conditions differ between ecologically distinct fish species. Journal of Experimental Biology, 221(22), jeb175281. https://doi.org/10.1242/jeb.175281

Lyall, A. H. (1957). Cone arrangements in teleost retinae. Journal of Cell Science. The Company of Biologists. https://journals.biologists.com/jcs/article/s3-98/42/189/64225/Cone-Arrangements-in-Teleost-Retinae

Mallatt, J., & Feinberg, T. E. (2021). Multiple routes to animal consciousness: Constrained multiple realizability rather than modest identity theory. Frontiers in Psychology, 12, 732336. https://doi.org/10.3389/fpsyg.2021.732336

Marshak, D. W. (2009). Retinal Ganglion Cells: Anatomy. In L. R. Squire (Ed.), Encyclopedia of Neuroscience (pp. 211–218). Academic Press. https://doi.org/10.1016/B978-008045046-9.00897-4

Marshall, N. J., Cortesi, F., de Busserolles, F., Siebeck, U. E., & Cheney, K. L. (2019). Colours and colour vision in reef fishes: Past, present and future research directions. Journal of Fish Biology, 95(1), 5–38. https://doi.org/10.1111/jfb.13849

Matthiessen, L. (1886). Ueber den physikalisch-optischen bau des auges der Cetaceen und der fische. Archiv für die gesamte Physiologie des Menschen und der Tiere, 38(1), 521–528. https://doi.org/10.1007/BF01654675

McFarland, W. N., & Munz, F. W. (1975). Part III: The evolution of photopic visual pigments in fishes. Vision Research, 15(10), 1071–1080. https://doi.org/10.1016/0042-6989(75)90003-6

McGuire, M., & Hill, J. (2021). SGEF 208/SG132: Invasive species of Florida's coastal waters: the red lionfish (*Pterois volitans*) and devil firefish *(P. miles)*. https://edis.ifas.ufl.edu/publication/SG132

Morris, J. A. (Ed.). (2012). Invasive lionfish: A guide to control and management. Gulf and Caribbean Fisheries Institute.

Morris, J. A., Akins, J. L., Barse, A., Cerino, D., Freshwater, D. W., Green, S. J., Muñoz, R. C., Paris, C., & Whitfield, P. E. (2008). Biology and ecology of the invasive lionfishes, *Pterois miles* and *Pterois volitans*. Gulf and Caribbean Fisheries Institute Conference, 61(7).

Nag, T. C., & Bhattacharjee, J. (1993). Retinal vascularization in the loach *Noemacheilus rupicola rupicola*: Coexistence of falciform process and vitreal vessels. Environmental Biology of Fishes, 36(4), 385–388. https://doi.org/10.1007/BF00012417

Nag, T. C., & Bhattacharjee, J. (2002). Retinal cytoarchitecture in Some mountain-stream teleosts of India. Environmental Biology of Fishes, 63(4), 435–449. https://doi.org/10.1023/A:1014982218347

Nelson, J. S., Grande, T. C., & Wilson, M. V. H. (2016). Fishes of the World. John Wiley & Sons.

Nicol, J. A. C. (1989). The eyes of fishes; Clarendon Press.

Nilsson, D.-E. (2009). The evolution of eyes and visually guided behaviour. Philosophical Transactions of the Royal Society B: Biological Sciences, *364*(1531), 2833–2847. https://doi.org/10.1098/rstb.2009.0083

Ogura, A., Ikeo, K., & Gojobori, T. (2004). Comparative analysis of gene expression for convergent evolution of camera eye between octopus and human. Genome Research, 14(8), 1555–1561. https://doi.org/10.1101/gr.2268104

Oh, I. K., Oh, J., Yang, K.-S., Lee, K. H., Kim, S.-W., & Huh, K. (2014). Retinal topography of myopic eyes: A spectral-domain optical coherence tomography study. Investigative Ophthalmology & Visual Science, 55(7), 4313–4319. https://doi.org/10.1167/iovs.14-14277

Pabón, P., & Acero, A. (2016). Ecología trófica del invasor pez león *Pterois volitans* en el Caribe colombiano: Impacto sobre familias ícticas de Santa Marta y San Andrés. Contribuciones En Ciencias Del Mar de La Universidad Nacional de Colombia, 74.

Pandarinath, C., Victor, J. D., & Nirenberg, S. (2010). Symmetry breakdown in the ON and OFF pathways of the retina at night: Functional implications. The Journal of Neuroscience, 30(30), 10006–10014. https://doi.org/10.1523/JNEUROSCI.5616-09.2010

Paxton, J. R., Eschmeyer, W. N., & Kirshner, D. (1998). Encyclopedia of Fishes. Academic Press.

Pettigrew, J. D., Dreher, B., Hopkins, C. S., McCall, M. J., & Brown, M. (1988). Peak density and distribution of ganglion cells in the retinae of microchiropteran bats: Implications for visual acuity (Part 2 of 2). Brain, Behavior and Evolution, 32(1), 48–56. https://doi.org/10.1159/000316042

Pimentel, D., Lach, L., Zuniga, R., & Morrison, D. (2000). Environmental and economic costs of nonindigenous species in the United States. BioScience, 50(1), 53. https://doi.org/10.1641/0006-3568(2000)050[0053:EAECON]2.3.CO;2

Potier, S., Mitkus, M., Bonadonna, F., Duriez, O., Isard, P.-F., Dulaurent, T., Mentek, M., & Kelber, A. (2017). Eye size, fovea, and foraging ecology in accipitriform raptors. Brain, Behavior and Evolution, 90(3), 232–242. https://doi.org/10.1159/000479783

Rapaport, D. H., & Stone, J. (1984). The area centralis of the retina in the cat and other mammals: Focal point for function and development of the visual system. Neuroscience, 11(2), 289–301. https://doi.org/10.1016/0306-4522(84)90024-1

Salem, M. A. (2016). Structure and function of the retinal pigment epithelium, photoreceptors and cornea in the eye of *Sardinella aurita* (Clupeidae, Teleostei). The Journal of Basic & Applied Zoology, 75, 1–12. https://doi.org/10.1016/j.jobaz.2015.12.001

Salis, P., Roux, N., Soulat, O., Lecchini, D., Laudet, V., & Frédérich, B. (2018). Ontogenetic and phylogenetic simplification during white stripe evolution in clownfishes. BMC Biology, 16(1), 90. https://doi.org/10.1186/s12915-018-0559-7

Santon, M., Bitton, P.-P., Harant, U. K., & Michiels, N. K. (2018). Daytime eyeshine contributes to pupil camouflage in a cryptobenthic marine fish. Scientific Reports, 8(1). https://doi.org/10.1038/s41598-018-25599-y

Santon, M., Münch, T., & Michiels, N. (2019). The contrast sensitivity function of a small cryptobenthic marine fish. Journal of Vision*, 19,* 1. https://doi.org/10.1167/19.2.1

Schneider, C. A., Rasband, W. S., & Eliceiri, K. W. (2012). NIH Image to ImageJ: 25 years of image analysis. Nature Methods, 9(7), Article 7. https://doi.org/10.1038/nmeth.2089

Shahidi, M., Blair, N. P., Mori, M., Gieser, J., & Pulido, J. S. (2002). Retinal topography and thickness mapping in atrophic age-related macular degeneration. British Journal of Ophthalmology, 86(6), 623–626. https://doi.org/10.1136/bjo.86.6.623

Shand, J. (1994). Changes in Retinal Structure during Development and Settlement of the Goatfish *Upeneus tragula*. Brain, Behavior and Evolution, 43(1), 51–60. https://doi.org/10.1159/000113624

Siebeck, U. E., Collin, S. P., Ghoddusi, M., & Marshall, N. J. (2003). Occlusable corneas in toadfishes: Light transmission, movement and ultrastruture of pigment during light- and dark-adaptation. Journal of Experimental Biology, 206(13), 2177–2190. https://doi.org/10.1242/jeb.00401

Spadea, L., Maraone, G., verboschi, francesca, Vingolo, E. M., & Tognetto, D. (2016). Effect of corneal light scatter on vision: A review of the literature. International Journal of Ophthalmology, 9. https://doi.org/10.18240/ijo.2016.03.24

Stieb, S., de Busserolles, F., Carleton, K., Cortesi, F., Chung, W.-S., Dalton, B., Hammond, L., & Marshall, N. (2019). A detailed investigation of the visual system and visual ecology of the Barrier Reef anemonefish, *Amphiprion akindynos*. Scientific Reports, 9, 16459. https://doi.org/10.1038/s41598-019-52297-0

Tamura, T., & Wisby, W. J. (1963). The visual sense of pelagic fishes especially the visual axis and accommodation. Bulletin of Marine Science, 13(3), 433–448.

Thetmeyer, H., & Kils, U. (1996). To see and not to be seen: The visibility of predator and prey with respect to feeding behaviour. Oceanographic Literature Review, 5(43), 472.

Thoreson, W. B., & Dacey, D. M. (2019). Diverse cell types, circuits, and mechanisms for color vision in the vertebrate retina. Physiological Reviews, 99(3), 1527–1573. https://doi.org/10.1152/physrev.00027.2018

Thorpe, A., Douglas, R. H., & Truscott, R. J. (1993). Spectral transmission and short-wave absorbing pigments in the fish lens—I. Phylogenetic distribution and identity. Vision Research, 33(3), 289–300. https://doi.org/10.1016/0042-6989(93)90085-b

Tikidji-Hamburyan, A., Reinhard, K., Storchi, R., Dietter, J., Seitter, H., Davis, K. E., Idrees, S., Mutter, M., Walmsley, L., Bedford, R. A., Ueffing, M., Ala-Laurila, P., Brown, T. M., Lucas, R. J., & Münch, T. A. (2017). Rods progressively escape saturation to drive visual responses in daylight conditions. Nature Communications, 8(1), Article 1. https://doi.org/10.1038/s41467-017-01816-6

Ullmann, J. F. P., Moore, B. A., Temple, S. E., Fernández-Juricic, E., & Collin, S. P. (2012). The retinal wholemount technique: A window to understanding the brain and behaviour. Brain, Behavior and Evolution, 79(1), 26–44. https://doi.org/10.1159/000332802

Ureña, H. M. (2009). El pez león del Indo-Pacífico: Nueva especie invasora en Costa Rica. Biocenosis, 22(1–2), Article 1–2. https://revistas.uned.ac.cr/index.php/biocenosis/article/view/1252

Wagner, H. J., Fröhlich, E., Negishi, K., & Collin, S. P. (1998). The eyes of deep-sea fish. II. Functional morphology of the retina. Progress in Retinal and Eye Research, 17(4), 637–685. https://doi.org/10.1016/s1350-9462(98)00003-2

Wagner, H.-J. (1990). Retinal structure of fishes. In R. Douglas & M. Djamgoz (Eds.), The Visual System of Fish (pp. 109–157). Springer Netherlands. https://doi.org/10.1007/978-94-009-0411-8_5

Walls, G. L. (1942). The vertebrate eye and its adaptive radiation (pp. xiv, 785). Cranbrook Institute of Science. https://doi.org/10.5962/bhl.title.7369

Warrant, E., & Locket, N. (2004). Vision in the deep sea. Biological Reviews of the Cambridge Philosophical Society, 79, 671–712. https://doi.org/10.1017/S1464793103006420

Webb, P. W. (1984). Body and fin form and strike tactics of four teleost predators attacking fathead minnow (*Pimephales promelas*) prey. Canadian Journal of Fisheries and Aquatic Sciences, 41(1), 157–165. https://doi.org/10.1139/f84-016

Whitfield, P. E., Hare, J. A., David, A. W., Harter, S. L., Muñoz, R. C., & Addison, C. M. (2007). Abundance estimates of the Indo-Pacific lionfish *Pterois volitans*/*miles* complex in the Western North Atlantic. Biological Invasions, 9(1), 53–64. https://doi.org/10.1007/s10530-006-9005-9

Whitfield, P., Gardner, T., Vives, S. P., Gilligan, M., Ray, W., Ray, G., & Hare, J. (2002). Biological invasion of the Indo-Pacific lionfish *Pterois volitans* along the Atlantic coast of North America. Marine Ecology Progress Series, 235, 289–297. https://doi.org/10.3354/meps235289

Wilby, D., & Roberts, N. W. (2017). Optical influence of oil droplets on cone photoreceptor sensitivity. Journal of Experimental Biology, jeb.152918. https://doi.org/10.1242/jeb.152918

Wood, R. W. (1911). Physical optics. New York: Macmillan. http://archive.org/details/physicaloptic00wood

Wool, L. E., Packer, O. S., Zaidi, Q., & Dacey, D. M. (2019). Connectomic identification and three-dimensional color tuning of S-OFF midget ganglion cells in the primate retina. Journal of Neuroscience, 39(40), 7893–7909. https://doi.org/10.1523/JNEUROSCI.0778-19.2019

Yamada, E., Bordt, A., & Marshak, D. (2005). Wide field ganglion cells in macaque retina. Visual Neuroscience, 22, 383–393. https://doi.org/10.1017/S095252380522401X

Yokoyama, S. (2008). Evolution of dim-light and color vision pigments. Annual Review of Genomics and Human Genetics, 9, 259–282. https://doi.org/10.1146/annurev.genom.9.081307.164228

7. APPENDICES

Appendix A**.** *Pterois volitans* Retinal Extraction Protocol (eyecup extraction). SL: Standard Length; HW: Head Width; CD: Corneal Diameter; TL: Corneal Transverse Length: AL: Corneal Axial Length; AG: Aphakip Gap ; ED: Lens Equatorial Diameter; TD: Lens Transverse Diameter

<table>
<tr><td colspan="3">Fish ID _____ Date_____
Collection site _____</td></tr>
<tr><td>Dark-adaptation</td><td colspan="2">Observations:</td></tr>
<tr><td>Anesthesia</td><td colspan="2">Observations:</td></tr>
<tr><td>Morphometry
Eye: R ___ L ___</td><td>SL _____
HW _____</td><td rowspan="4">Photo labels:</td></tr>
<tr><td>Enucleation</td><td>CD _____ TL _____
AL _____ AG _____
Observations: _____
_____</td></tr>
<tr><td>Eyeball hemisection</td><td>ED _____
TD _____
Observations: _____
_____</td></tr>
<tr><td>Fixation</td><td>PFA fixation time: _____
Washing 1 min x 3 ___ ___ ___
Container label: _____</td></tr>
</table>

Appendix B. *Pterois volitans* Retinal Extraction Protocol (retinal wholemount)

Experimenter _____ Date_____ Fish ID _____ Eye left ___ right ___	
Retinal extraction	Radial cuts _____ Observations:
Bleaching	Reagent _____ Initial-final time _____ Duration _____ Observations: Rinsed x3 in PBS ___
Wholemount	Flatten retina _____ Mount in glycerol _____ Seal (nail varnish) _____ Label slide_____
Observations:	

Appendix C. Nissl Stain Protocol Applied to Lionfish Retinae

Stage	**Reagent**	**Time**
1	acid acetone (1:1 glacial acetic acid and acetone)	5 min
2	distilled water	1 min
3	0.1% Cresyl violet	10 min
4	10% glacial acetic acid	1 min
5	Acetone	15 s
6	Acetone	30 s
7	Xylene	1 min
8	xylene	1 min

Appendix D**.** Construction of a Retinal Map with R Package “Retina”

Figure 17 D1. Wide view (a) and close view (b) of retinal outline with pre-set coordinates and cell counts in each counting point.

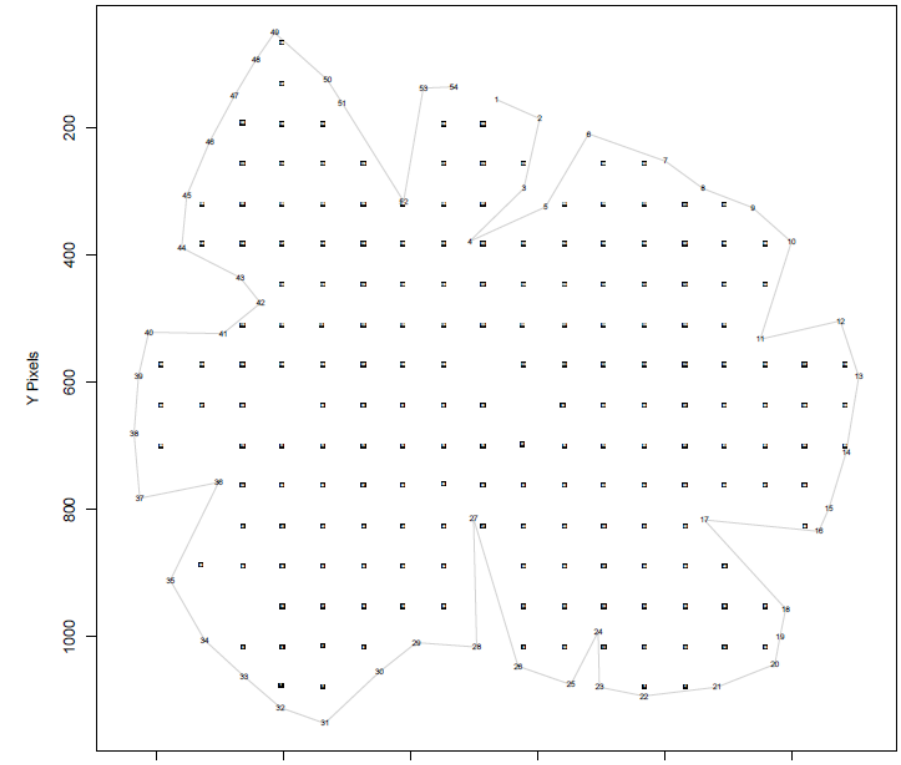

a.

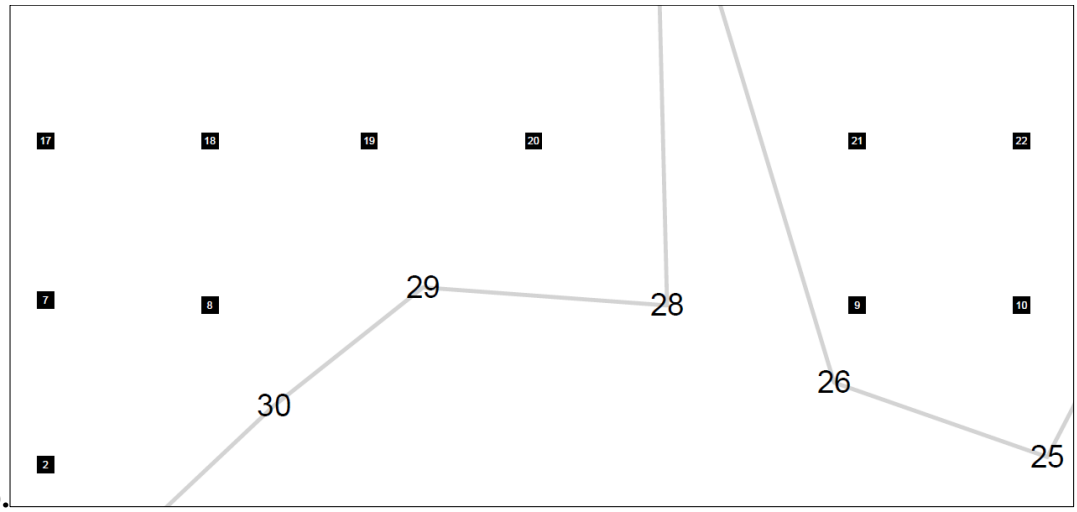

b.

Appendix D (cont.). Construction of a Retinal Map With R Package “Retina”

Figure 18 D2. Retinal outline with color legend representing cell densities.

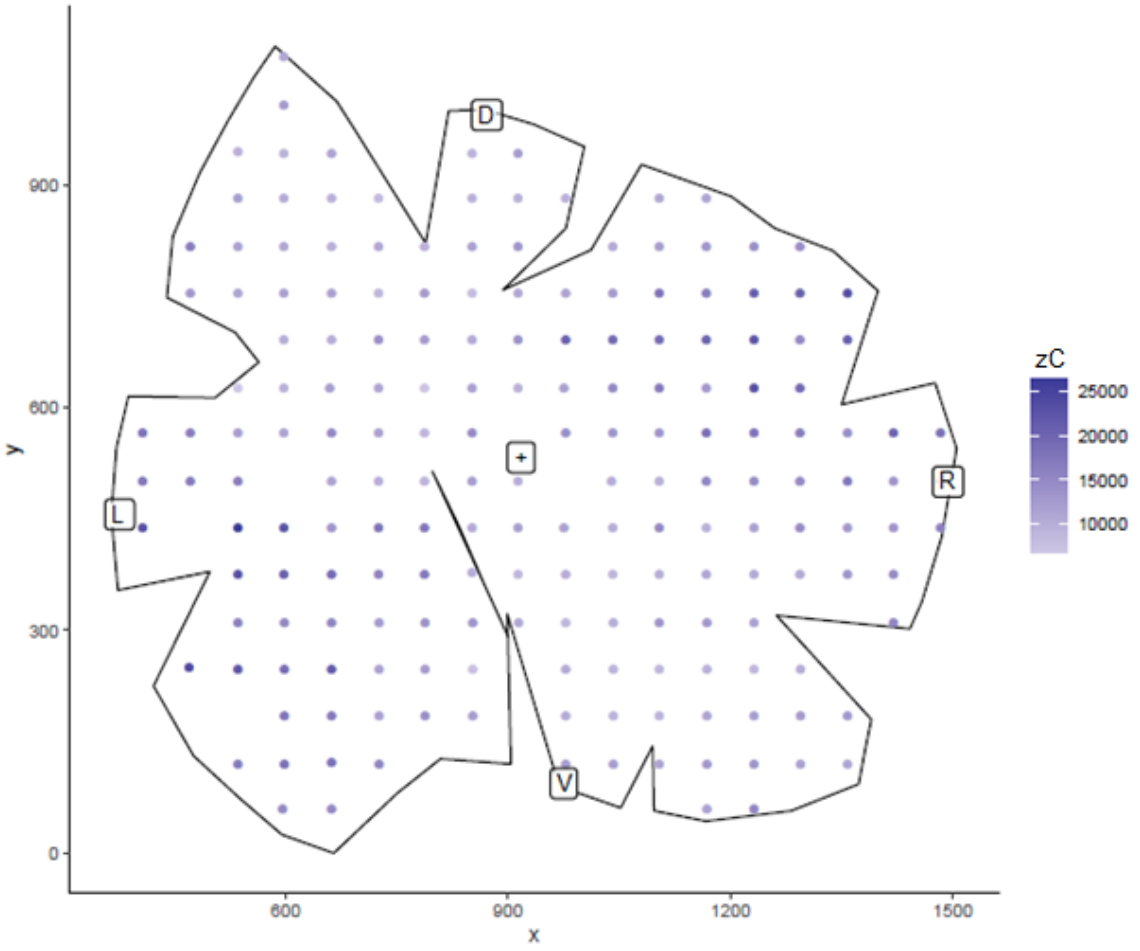

Appendix E**.** Equations to Calculate Spatial Resolving Power for Teleosts

Posterior nodal distance PND	PND = 2.55 x r
Angle (α) subtending 1 mm on the retina	α = arc tan 1 mm/PND
Spatial resolving power	cells per degree = density at area of peak cell distribution / PND
	cycles per degree = cells per degree / 2

Appendix F**.** Red Lionfish in Their Natural Environment

Figure 19 F1. Red Lionfish Specimens Observed during Midday Hours at “Ciénaga de los Vásquez” Underwater Museum, Barú Island, Colombian Caribbean. Photo Credit: Javier Torres.